*Prog. Oceanog.* Vol. 27, pp. 365-402, 1991.
Printed in Great Britain. 

0079 - 6611/91 $0.00 + .50


# A numerical ocean circulation model of the Norwegian and Greenland Seas

DAVID P. STEVENS

*School of Mathematics, University of East Anglia, Norwich NR4 7TJ, UK*

**Abstract** – The dynamics and thermodynamics of the Norwegian and Greenland Seas are investigated using a three-dimensional primitive equation ocean circulation model. The horizontal resolution of the model is 1° in the zonal direction and 0.5° in the meridional direction. The vertical structure is described by 15 levels. The model is driven by both annual mean and seasonally varying wind and thermohaline forcing. The connections of the Norwegian and Greenland Seas with the North Atlantic and Arctic Ocean are modelled with an open boundary condition. The simulated currents are in reasonable agreement with the observed circulation.

CONTENTS



## 1. INTRODUCTION

The Norwegian and Greenland Seas situated between Norway and Greenland are bounded to the south by the Greenland Scotland ridge and to the north by Spitsbergen (Svalbard) and the Fram strait. There are two main basins in the region, the Norwegian basin in the south and the Greenland basin to the north. There are many interesting and complex oceanographic phenomena taking place in the region. Warm saline water flows into the region from the North Atlantic between the Shetland Isles and the Faroes. As this water is advected north it is cooled and becomes more dense. The Greenland Sea is an area of intense cooling where the surface waters are cooled so much that the water column becomes unstable and overturns forming bottom water. Various authors have speculated on how bottom water is formed. CARMACK and AAGAARD (1973) propose a sub-surface modification of the North Atlantic water in the Greenland gyre based on a double diffusive process. KILLWORTH (1979) suggests formation by "chimneys", narrow

regions of intense mixing to great depths. There is also the possibility that deep water is formed during the process of ice formation. Dense water formed in the Norwegian and Greenland Seas overflows the Greenland-Scotland ridge system into the North Atlantic forming its deep water. In fact this is a major driving force of the North Atlantic thermohaline circulation. To the west along the Greenland coast there is a strong current of cold fresh water, the East Greenland Current, which originates in the Arctic. WORTHINGTON (1970) provides budgets for mass transport and heat. The warm water which flows up from the North Atlantic gives up its heat to the atmosphere which is largely responsible for keeping the climate of northwestern Europe anomalously warm. The wind forcing produces a largely cyclonic circulation over the Norwegian and Greenland Sea basins (AAGAARD, 1970). Sea ice is formed in the region, mainly to the west and north of the area modelled. This can have important consequences for the climate, as the interaction between the atmosphere and ocean is considerably changed in the presence of sea ice. There is a distinct lack of observations in the region (especially in winter) mainly because of the inhospitable weather. Unfortunately there is a lack of quality surface boundary data which are essential to realistically simulate the thermohaline circulation.

The forefathers of research into the Norwegian and Greenland Seas were HELLAND-HANSEN and NANSEN. Their much quoted 1909 report "The Norwegian Sea" includes their schematic of the surface circulation which has appeared in a number of publications (Fig.1, taken from METCALF, 1960). LEE (1963) reviews much of the work done to that time. More recently an excellent comprehensive review of the physical oceanography and literature has been produced by HOPKINS (1988)

The previous effort in modelling the Norwegian and Greenland Seas is very limited. CREEGAN (1976) uses a two layer model with inflow from the North Atlantic through the Faroe-Shetland channel and a corresponding outflow through the Fram strait. This outflow is almost certainly too large compared with mass transport budgets of WORTHINGTON (1970). The poor thermodynamics of the model do not allow cooling of Atlantic water and formation of bottom water. The model also completely neglects the East Greenland Current. However, the model does quite well in quantitatively predicting the gross features of the wind driven circulation, including the mainly cyclonic circulation over each basin. A simple box model is employed by PETERSON and ROOTH (1976) who argue that bottom water is formed mainly in the Greenland Sea and that deep water in the Norwegian Sea comes mainly from the Greenland Sea. Using bomb test tritium and radiocarbon data they calculate that the timescale for deep convective mixing in the Greenland Sea is approximately 30 years and the timescale for the exchange between the deep Greenland Sea and deep Norwegian Sea is at least 100 years.

SEMTNER (1976b) includes the Norwegian and Greenland Seas in one of his Arctic Ocean simulations. The grid size of 110km that he uses is rather large. The surface wind and salinity forcing are annual means. A seasonally varying but spatially constant heat flux is also applied. SEMTNER prescribes variables from observations at open boundaries, using steady mean values. The resulting circulation along with temperature and salinity fields seems to be in general agreement with observations. More recently HIBLER and BRYAN (1987) have studied the same region as SEMTNER with a coupled ice-ocean model using seasonal thermal forcing and daily wind stresses of 1979. The ocean part of their model is largely diagnostic as the temperature and salinity fields below the mixed layer are not allowed to drift too far away from climatology. Open boundaries are treated in the following way; solid walls enclose the region that is modelled and thus no mass transport can be prescribed across these "open boundaries". The temperature and salinity fields are forced to climatology on a 30 day time scale. This results in intense vertical circulation close to the boundary although they claim these walls are away from the region of

interest and have little effect on the flow there. SEMTNER (1987) extended his 1976 model by including more realistic surface forcing and a sea ice model. The predicted currents in the above three models are rather low. This is because of the excessively large eddy viscosities used for computational stability. Finally, the work of LEGUTKE (1986) must be noted, although only a limited amount has yet been published. She uses a similar approach to that used here although the horizontal resolution is higher and the domain of interest is slightly smaller. [Ed: see this issue.]

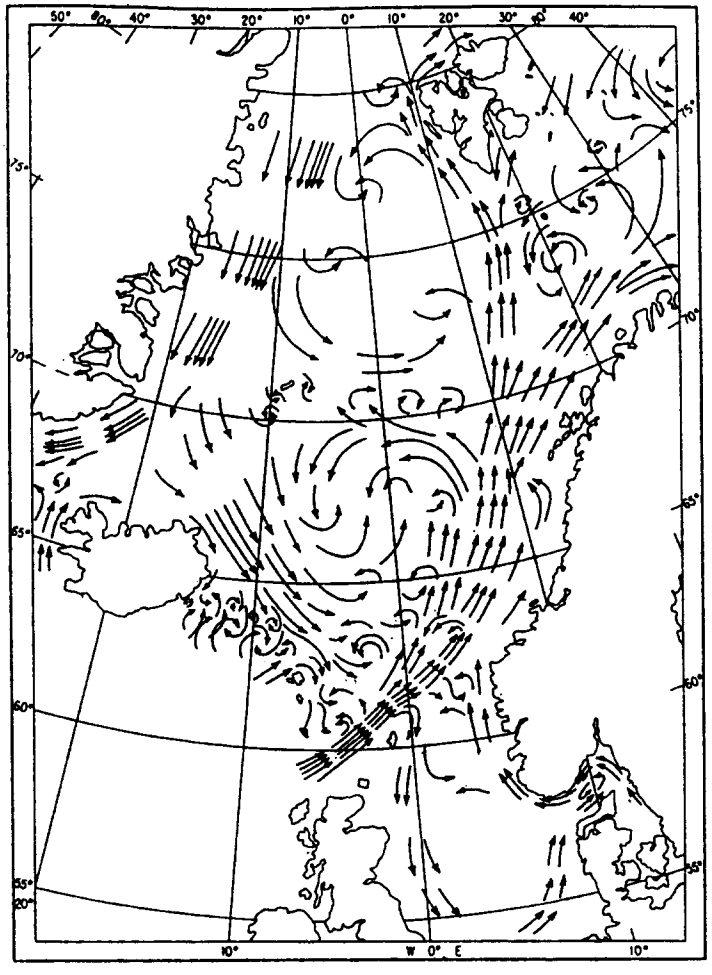


FIG.1. Schematic of the surface circulation taken from METCALF (1960).

## 2. THE NUMERICAL MODEL

The ocean general circulation model used in this study is based on that of COX (1984). This is one of a number of models whose origin can be traced back to the pioneering work of BRYAN (1969). The equations describing motion, temperature and salinity are solved using a finite difference formulation. The full equations are:

$$\frac{\partial u}{\partial t} + \Gamma(u) - fv = -\frac{1}{\rho_0 a \cos\phi}\frac{\partial p}{\partial \lambda} + K_m\frac{\partial^2 u}{\partial z^2} + A_m\left(\nabla^2 u + \frac{(1-\tan^2\phi)u}{a^2} - \frac{2\sin\phi}{a^2\cos^2\phi}\frac{\partial v}{\partial \lambda}\right), \quad (1)$$

$$\frac{\partial v}{\partial t} + \Gamma(v) + fu = -\frac{1}{\rho_0 a}\frac{\partial p}{\partial \phi} + K_m\frac{\partial^2 v}{\partial z^2} + A_m\left(\nabla^2 v + \frac{(1-\tan^2\phi)v}{a^2} + \frac{2\sin\phi}{a^2\cos^2\phi}\frac{\partial u}{\partial \lambda}\right), \quad (2)$$

$$\frac{\partial p}{\partial z} = -\rho g, \quad (3)$$

$$\Gamma(1) = 0, \quad (4)$$

$$\frac{\partial T}{\partial t} + \Gamma(T) = K_h\frac{\partial^2 T}{\partial z^2} + A_h\nabla^2 T, \quad (5)$$

$$\rho = \rho(\theta, S, z) \quad (6)$$

where

$$\Gamma(\mu) = \frac{1}{a\cos\phi}\frac{\partial}{\partial\lambda}(u\mu) + \frac{1}{a\cos\phi}\frac{\partial}{\partial\phi}(v\mu\cos\phi) + \frac{\partial}{\partial z}(w\mu),$$

and

$$\nabla^2(\mu) = \frac{1}{a^2\cos^2\phi}\frac{\partial^2\mu}{\partial\lambda^2} + \frac{1}{a^2\cos\phi}\frac{\partial}{\partial\phi}\left(\frac{\partial\mu}{\partial\phi}\cos\phi\right).$$

The variables $\phi$, $\lambda$, z, u, v, w, p, $\rho$ represent latitude, longitude, depth, zonal velocity, meridional velocity, vertical velocity, pressure and density respectively. The radius of the Earth is a, g is the acceleration resulting from gravity, $\rho_0$ is a reference density and $f = 2\Omega \sin\phi$ is the Coriolis parameter where $\Omega$ is the Earth's angular speed of rotation. The variable T represents any tracer including active tracers such as potential temperature $\theta$ and salinity S or passive tracers such as tritium. The nonlinear equation of state (6) gives density as a function of potential temperature $\theta$, salinity S and depth z. The equation is approximated by a polynomial fit to the Knudsen formulae as described by BRYAN and COX (1972). $A_m$ and $A_h$ are the horizontal mixing coefficients for momentum and tracers. $K_m$ and $K_h$ are the corresponding vertical mixing coefficients. Although the above equations are referred to as "primitive equations" some approximations have already been made, namely that the fluid is hydrostatic, Boussinesq and incompressible. As convective mixing cannot occur in a hydrostatic model such as this, some form of parameterisation must be used to take account of it. If the water column becomes statically unstable it is instantaneously mixed to produce a stable water column.

The equations of motion are rearranged to form an equation for the barotropic stream function $\upsilon$:

$$\left[\frac{\partial}{\partial\lambda}\left(\frac{1}{H\cos\phi}\frac{\partial^2\psi}{\partial\lambda\partial t}\right)+\frac{\partial}{\partial\phi}\left(\frac{\cos\phi}{H}\frac{\partial^2\psi}{\partial\phi\partial t}\right)\right]-\left[\frac{\partial}{\partial\lambda}\left(\frac{f}{H}\frac{\partial\psi}{\partial\phi}\right)-\frac{\partial}{\partial\phi}\left(\frac{f}{H}\frac{\partial\psi}{\partial\lambda}\right)\right]$$
$$=-\left[\frac{\partial}{\partial\lambda}\left(\frac{g}{\rho_0 H}\int_{-H}^{0}\int_{z}^{0}\frac{\partial\rho}{\partial\phi}\,dz'\,dz\right)-\frac{\partial}{\partial\phi}\left(\frac{g}{\rho_0 H}\int_{-H}^{0}\int_{z}^{0}\frac{\partial\rho}{\partial\lambda}\,dz'\,dz\right)\right]$$
$$+\left[\frac{\partial}{\partial\lambda}\left(\frac{a}{H}\int_{-H}^{0}F^{v}-\Gamma(v)\,dz\right)-\frac{\partial}{\partial\phi}\left(\frac{a\cos\phi}{H}\int_{-H}^{0}F^{u}-\Gamma(u)\,dz\right)\right] \tag{7}$$

where

$$-\frac{1}{a}\frac{\partial\psi}{\partial\phi}=\int_{-H}^{0}u\,dz,\quad \frac{1}{a\cos\phi}\frac{\partial\psi}{\partial\lambda}=\int_{-H}^{0}v\,dz$$

and $F^u$, $F^v$ are the diffusive terms on the right hand side of equations (1), (2) respectively.

Details of the equations for the baroclinic velocities and the method of solution have been given by various authors (BRYAN, 1969; SEMTNER, 1974; COX, 1984; and SEMTNER, 1986). The finite difference grid used is that of the Arakawa "B" type, in which tracer points T and stream function points $\psi$ are placed in the centre of cells and the horizontal velocity components u, v are situated at the corners. In the vertical T, u, v are located in the centre of the cell. Time stepping is achieved by leapfrogging, with the associated time splitting removed by a Robert time filter as described by ASSELIN (1972).

At the surface the model is driven by a prescribed wind stress and buoyancy forcing. The usual no slip and no flux of tracer conditions are applied at lateral boundaries. A no flux of tracer condition is specified at the ocean floor. A further condition at the ocean floor is that of bottom friction, which is applied through a square law with a drag coefficient of $1.3\times10^{-3}$ and a 10° turning angle resulting from Ekman effects. Further details of the boundary conditions applicable at natural land boundaries have been given in the above four articles.

The boundary condition at open ocean boundaries is based on that of STEVENS (1990). This method calculates variables at the boundary from dominant terms in the governing equations. The baroclinic velocity field is determined from the momentum equations (1) and (2) with two modifications. Firstly the nonlinear terms which are small throughout much of the ocean are neglected. Secondly the unknown value in the diffusion term (which lies outside the model domain) is approximated by the value on the boundary. The treatment of tracers depends upon whether there is inflow or outflow at a point on the boundary at a given time. At inflow points information propagates inwards from a region which is not modelled, so tracers are relaxed to observed values. At points where there is either advection or wave propagation outwards, tracers are calculated from terms involving that advection or wave propagation normal to the boundary and a diffusion term which is modified in a similar way to that in the momentum equations. The calculation of the stream function at open boundaries provides the greatest difficulty. There are no tractable simplications to the equation (7) describing the stream function $\psi$ that are generally applicable. The choice of boundary condition for the stream function is discussed in section 4.

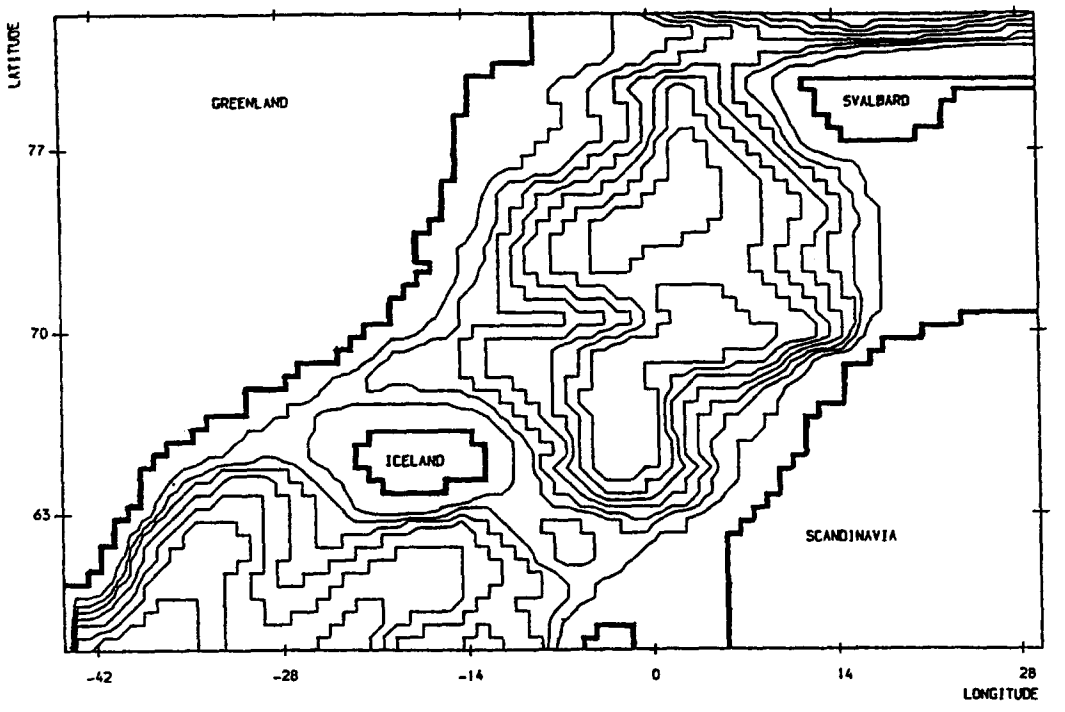


FIG.2. The model domain and topography.

## 3. THE MODEL DOMAIN, GRID AND PARAMETERS

The area to be modelled along with the resolved topography is illustrated in Fig.2. The region extends from 57.5° to 82.5°N and from 45°W to 30°E. The area includes both the Norwegian and Greenland basins and extends past the sills and straits separating them from the adjoining oceans. Topographic data are obtained from the LEVITUS (1982) dataset. A look at any bathymetric chart indicates that the smooth model topography only resolves the large scale features of the region.

The horizontal grid spacing is 0.5° in the meridional direction and 1° in the zonal direction. This gives a spacing of approximately 55km in the meridional direction and a spacing that varies from 59km in the south to 16km in the north, in the zonal direction. This variation results from the convergence of the meridians toward the North Pole. The spacing is unable to resolve eddies, however, it is the best that can be achieved with the computational facilities available. The size of the resulting horizontal grid is 76 by 51 grid points. There are 15 levels in the vertical with thicknesses of 10, 20, 40, 60, 80, 100, 130, 160, 200m, the remaining grid boxes are 400m thick. Most of the resolution is near the surface, where the main structure in the ocean occurs. The deeper boxes could be thicker but are kept at 400m to resolve variations in the bottom topography.

As calculations of variables are made at land as well as sea points (for the purpose of vectorisation of the model code) it is important to reduce the land area within the domain of interest. Thus the model domain is rearranged so that the region east of 8°E is placed inside Greenland for the purpose of calculations. The area of "wasted" land is much reduced. The size

of the horizontal grid is reduced from 76 by 51 points to 54 by 51 points, this increases computational efficiency and reduces storage requirements.

Vertical mixing in the ocean is still poorly understood and poorly treated in general circulation models. The vertical mixing coefficients $K_m$ and $K_h$ are not limited by any stability criteria for any realistic range of values. For this study a simplistic approach is taken. A constant value of $1 cm^2 s^{-1}$ is used for both $K_m$ and $K_h$. There is no doubt that this value is rather large for the more stably stratified regions of the ocean and probably too small for the less stratified waters, but nevertheless it provides a compromise.

A realistic value for $A_m$ is of the order of $10^6 cm^2 s^{-1}$. However, $A_m$ has to be chosen large enough to eliminate computational noise (a common problem with large scale primitive equation models) and thus its value is dictated by the grid size. Details of stability criteria have been given by various authors, for instance BRYAN, MANABE and PACANOWSKI (1975) and KILLWORTH, SMITH and GILL (1984). The value of $A_m$ used in this study is $10^8 cm^2 s^{-1}$. The stability criteria on the horizontal diffusivity $A_h$ are not quite so severe, a more realistic value of $10^7 cm^2 s^{-1}$ is used.

Finally the length of timesteps needs to be decided. The convergence of the meridians to the north means that the diffusive condition is the most restrictive, namely

$$\Delta t < \frac{\Delta^2}{8A_m},$$

where $\Delta t$ is the timestep and $\Delta$ is the width of the smallest grid box. This timestep limitation is well known and can be found in almost any text on numerical analysis, for example O'BRIEN (1986). Under the above condition a maximum timestep of 2900 seconds is allowed. However, for this study a timestep of 2700 seconds (45 minutes) is used.

## 4. ANNUAL MEAN FORCING

In this section annual mean surface forcing is used to drive the model ocean. The temperature and salinity fields throughout the model ocean are initialised using the LEVITUS (1982) climatology, whilst the velocity fields are started from rest. The initial density at the surface and the temperature and salinity fields at 520m are shown in Fig.3. Warm saline water of North Atlantic origin can be seen off the Norwegian coast. The fresh surface water at the coast is caused by fresh water runoff from rivers and fjords. To the west (off the Greenland coast) cold fresh East Greenland Current water of Arctic origin is apparent. The densest water occurs over the Greenland Sea basin. A further point of note is the smooth nature of the data.

The surface wind stress is obtained from 12 hourly NMC (National Meteorological Centre, USA) wind velocities for 1982, which are stored in 2.5° latitude longitude squares. The wind stress is calculated from the wind velocity using the following empirical formulae

$$\tau^{\lambda} = \rho_a c_d u_w |v_w|, \; \tau^{\phi} = \rho_a c_d v_w |v_2|, \tag{8}$$

where $\rho_a$ is the density of air, $c_d$ is a drag coefficient and $v_w$ is the wind velocity vector with components $u_w$ and $v_w$. The relationship (8) has been used by many authors (for example GILL, 1982, p.29; SEMTNER, 1976b) with various formulae for the drag coefficient $c_d$, which is obtained by fitting experimental data. For this study the linear relationship of ANDERSON (personal communication)

$$c_d = 0.013(0.8 \;\; 0.065|v_2|),$$

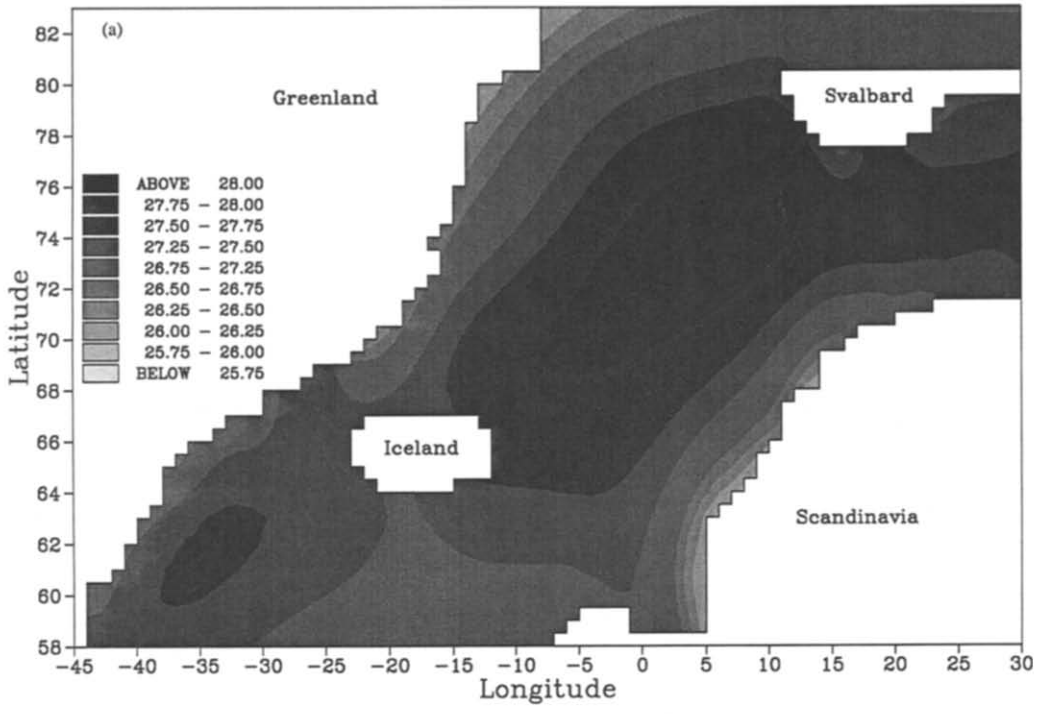
(a)
Greenland
Svalbard
Iceland
Scandinavia
ABOVE 28.00
27.75 – 28.00
27.50 – 27.75
27.25 – 27.50
26.75 – 27.25
26.50 – 26.75
26.25 – 26.50
26.00 – 26.25
25.75 – 26.00
BELOW 25.75
Latitude
Longitude

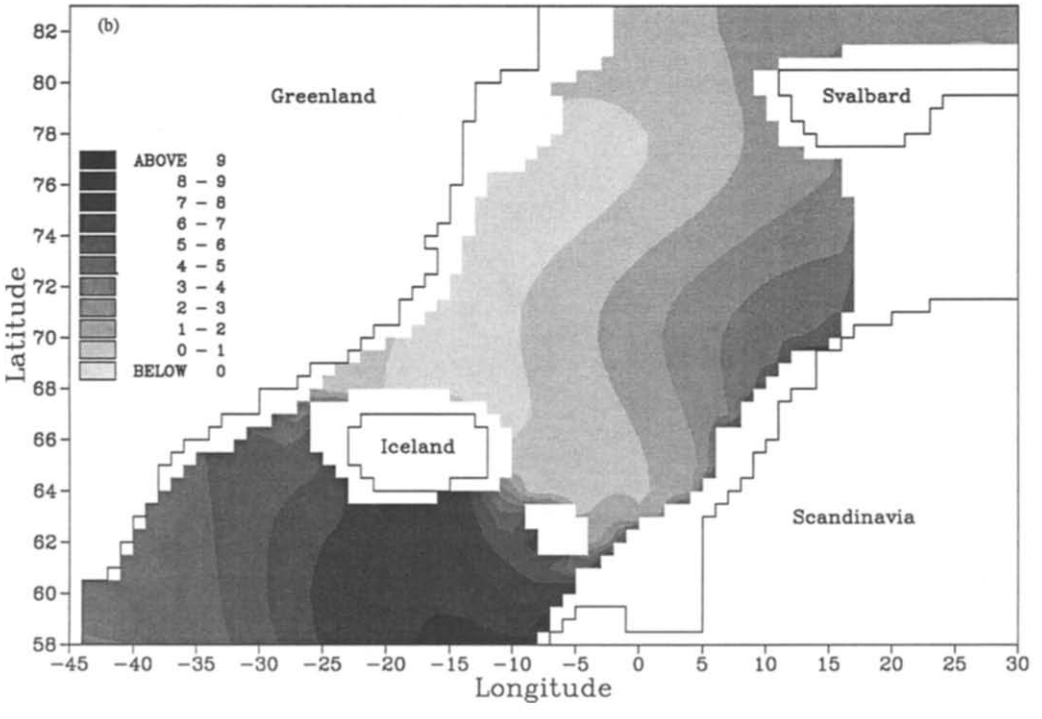
(b)
Greenland
Svalbard
Iceland
Scandinavia
ABOVE 9
8 – 9
7 – 8
6 – 7
5 – 6
4 – 5
3 – 4
2 – 3
1 – 2
0 – 1
BELOW 0
Latitude
Longitude

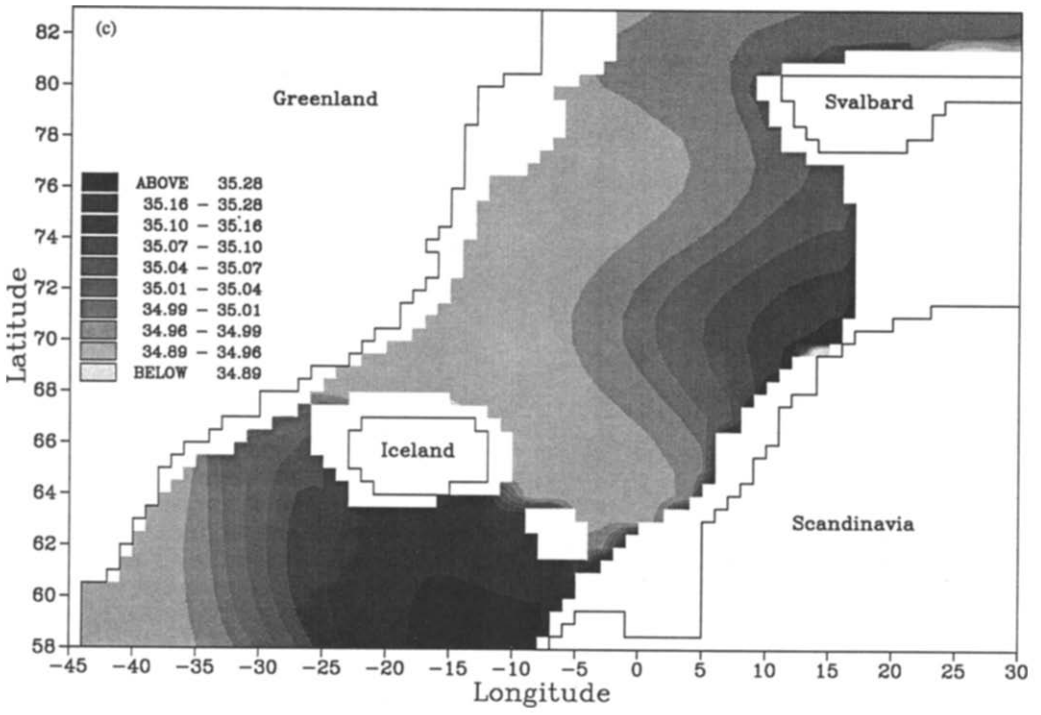


FIG.3. Annual mean (a) surface density (kg $m^{-3}$-1000), (b) temperature (°C) at 520m, and (c) salinity (ppt) at 520m.

is used. The wind stresses are then averaged to produce an annual mean. Finally the wind stresses are interpolated from the 2.5° latitude, longitude grid onto the model grid using a bi-cubic spline interpolation procedure. Figure 4 shows the 1982 annual mean. The prominent cyclonic structure of the wind is clearly illustrated. South-westerlies blow northward past Scotland and Norway, whilst winds of polar origin blow southward adjacent to Greenland. This annual mean pattern is very representative of the wind, except for a few short spells in the spring and summer.

There is a choice of surface boundary conditions on tracers between prescribing values of temperature and salinity at the surface or specifying a flux. A flux condition is certainly the more pleasing condition to use, for in reality the ocean is driven by fluxes. It also allows the ocean surface waters far more freedom than prescribing tracers at the surfae. However data for the region are sparse so the surface temperature and salinity are prescribed from annual mean LEVITUS (1982) data. The specification of surface values is used in the hope of making the model more realistic in the absence of reliable flux data. In fact prescribing tracer values on the surface level of such a model can almost be thought of as specifying a flux condition on the level below. Prescribing the surface value of salinity also has the advantage that the shallow coastal waters are continually kept fresh by the imposed data, thus retaining the effect of freshwater river runoff.

The final point to consider is the boundary data that needs to be fed into the open boundaries of the model. For the runs described in this article, the southern boundary is open between 45°W and 7°W, while the northern boundary is open between 4°W and 30°E. The only substantial sea

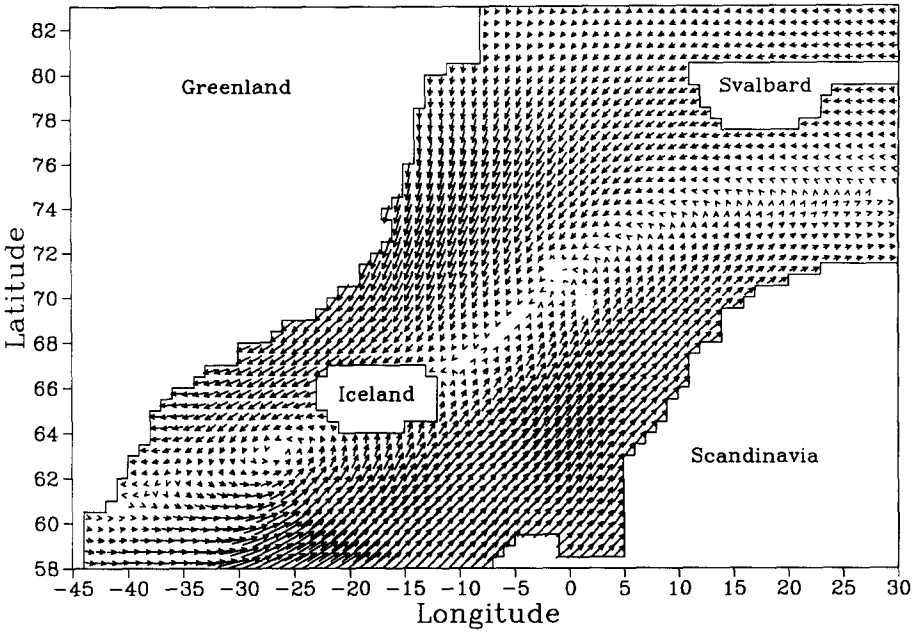


FIG.4. The 1982 annual mean wind stress. The distance between grid points corresponds to a stress of $0.2 Nm^{-2}$.

boundary that remains closed is that separating the eastern half of the Barents Sea from the model domain. This is a very shallow region and any transports are likely to be small, a view which is supported by AAGAARD and GREISMAN (1975). The temperature and salinity for the open boundary condition is specified from the LEVITUS (1982) data.

Providing a condition for the stream function at open boundaries is quite a challenge. STEVENS (1990) shows that a simple radiation condition can be appropriate at an unforced boundary. However, in the case considered here, there is forcing at both boundaries. STEVENS also shows that the Sverdrup balance can give a good approximation in certain situations. If stratification is included and there is no variation in topography, then there is very little interaction between the barotropic and baroclinic modes. In this case the Sverdrup relation is appropriate. However if topography and stratification are both included then the baroclinic mode forces and changes the barotropic mode through the bottom pressure torque. In some cases stratification can greatly reduce the effect of topography (see ANDERSON and KILLWORTH, 1977), but in the situation considered here the bottom pressure torque has a large effect on the barotropic component of the flow and thus the Sverdrup balance is not applicable.

One reasonable approach is to specify the stream function from observations. As a result of the lack of available data it was decided that the exchange of fluid at open boundaries should take place at four strategically chosen locations. These are the main regions of exchange with the surrounding seas described by WORTHINGTON (1970). The regions are marked in Fig.5. Region A is the inflow from the North Atlantic, region B is the outflow into the Arctic Ocean, region C is the inflow from the Arctic Ocean and region D is the outflow into the North Atlantic. The transports through each gap are taken from the estimates of WORTHINGTON (1970). The actual values used in the model are 13 Sverdrups inflow through gap A and a similar outflow through

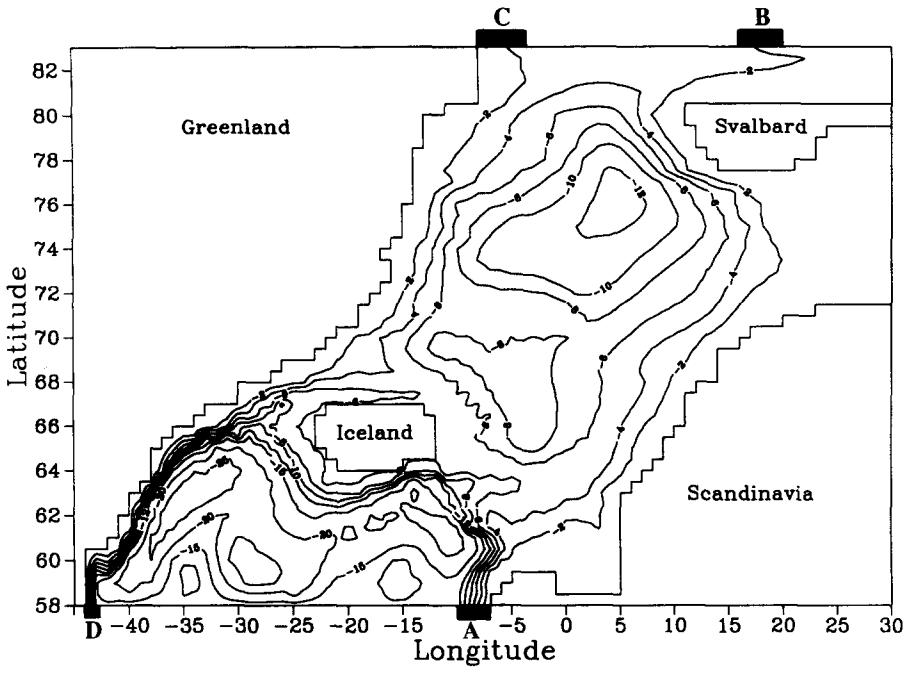


FIG.5. The stream function (in Sverdrups) after 1000 timesteps (31 days) using the estimates of WORTHINGTON (1970) for stream function boundary data. The contour interval is 2 Sverdrups between -2 and -12 Sverdrups and 5 Sverdrups for values less than -15 Sverdrups.

gap D in the south. While an exchange of 3 Sverdrups, outflow through gap B and inflow through gap C, took place with the Arctic Ocean. The large value of 13 Sverdrups inflow from the North Atlantic rather than the 8 Sverdrups suggested by Worthington is to compensate for the blocking effect of the Iceland-Scotland ridge. It was found that most of the water that was input through gap A would turn westwards, south of Iceland and head towards outflow D.

A run was performed using the boundary data described above. The resulting stream function field at 1000 timesteps (31 days) is shown in Fig.5. The inflow from the North Atlantic splits into two parts with one travelling northwards into the Norwegian Sea and the other heading westward to the south of Iceland. There is a region of cyclonic circulation over the Greenland Sea basin and a similar region of weaker circulation over the Norwegian Sea basin. With reference to Fig.2 it can be seen that the circulation is strongly controlled by topography. The circulation within the Norwegian and Greenland Seas looks reasonably realistic. However the same cannot be said of the region to the south of Iceland. There are a number of small strong gyres and a region of strong flow tangential to the southern boundary. Also large vertical velocities occur in the region close to the southern boundary. The main driving force of the barotropic flow in this region is the bottom pressure torque. It seems that this unphysical and undesirable behaviour of the stream function is brought about by the unsatisfactory boundary condition at the southern boundary. The boundary data are not consistent with the topography and the density field which forces the stream function. Thus the use of a few small regions for exchanges of water between ocean basins (and effectively what is a solid wall to the barotropic mode elsewhere) seems to be limited. This is especially so at the southern boundary where major exchanges of water masses take place. No such problems occur at the northern boundary where exchanges with the Arctic Ocean are on a much smaller scale. The stream function here is able to adjust within a single grid point from the

approximate boundary data to a value consistent with the equations of motion. As the behaviour of the northern boundary gives no cause for concern the condition here will be retained, whilst a new approach will be sought at the southern boundary.

Various forms of extrapolation (from interior grid points) have been tested. However these all produce similar types of unphysical behaviour (when they remain stable). The stream function field away from the southern boundary is always similar to that of Fig.5. Thus the difference in boundary condition has little effect on the circulation in the Norwegian and Greenland Seas over the short period of integration used here. This may not be true over a longer time scale.

Finally some stream function "data" for the southern boundary are created by running a smaller model which surrounds that boundary. The model stretches 7.5° either side of the southern boundary of the Norwegian and Greenland Seas model (57.5°N). All surrounding boundaries are closed, as they are far enough from 57.5°N as to have no significant affect. The model has the same grid spacing and parameters as the Norwegian and Greenland Seas model and is initialised and forced as in the previous experiment. The model is then spun up for 2 months. This allows time for the barotropic field to respond to the forcing and stratification. The stream function along 57.5°N is then noted. The Atlantic inflow to the west of Scotland is increased to 8 Sverdrups to be consistent with WORTHINGTON (1970). The fact that there is a broad northward flow across much of the southern boundary removes the need to increase the inflow further. Mass is conserved by increasing the western boundary current off Greenland by a corresponding amount. The data are now largely consistent with the stratification and topography.

With the inclusion of this improved stream function boundary data the model is run for a period of five years. This is a long enough time for the model to settle down from the initial start up shock and spin up the surface and intermediate waters. For comparison with Fig.5 the stream function at 1000 timesteps is illustrated in Fig.6. It can be seen that none of the gyres adjacent to, and strong currents tangential to, the boundary that featured in previous runs are present. Further unlike previous runs large vertical velocities close to the boundary are absent. The stream function data at the boundary are consistent with the forcing, density field and topography, and thus no unphysical or unrealistic looking flows are produced. Figure 7 illustrates the near surface (20m) velocity after five years. The circulation over the Norwegian and Greenland Sea basins is largely cyclonic. The major known surface currents such as the East Greenland Current, East Icelandic Current, West Spitsbergen Current and Norwegian Current are all reproduced by the model and can be clearly identified.

Figure 8 shows the stream function after five years. The strength of the gyre over the Norwegian Sea basin has increased considerably. The gyre over the Greenland Sea basin has increased slightly in strength, while its centre has moved southwards almost merging with the Norwegian Sea gyre. Associated with this change in the stream function is an increase in temperature and thus a drop in density of the intermediate waters. However the salinity field remains relatively unchanged. The temperature increase is greatest over the Greenland Sea basin, where differences from the initial state of more than 3°C occur. The entire structure of the density field within the Norwegian and Greenland Seas changes. The most dense water occurs over the Norwegian Sea basin, where the density field enhances the cyclonic circulation. The increase in temperature in the Greenland Sea is brought about by the northward advection of warm North Atlantic water and the lack of cooling and convective mixing which is usually present. The use of annually averaged thermohaline forcing means that the surface waters do not reach the winter time minimum temperatures and maximum densities that occur in reality. The water column remains stable. Therefore convective mixing, which transmits these minima and maxima of temperature and density to the deeper water, does not occur. It is the doming up of isopycnals

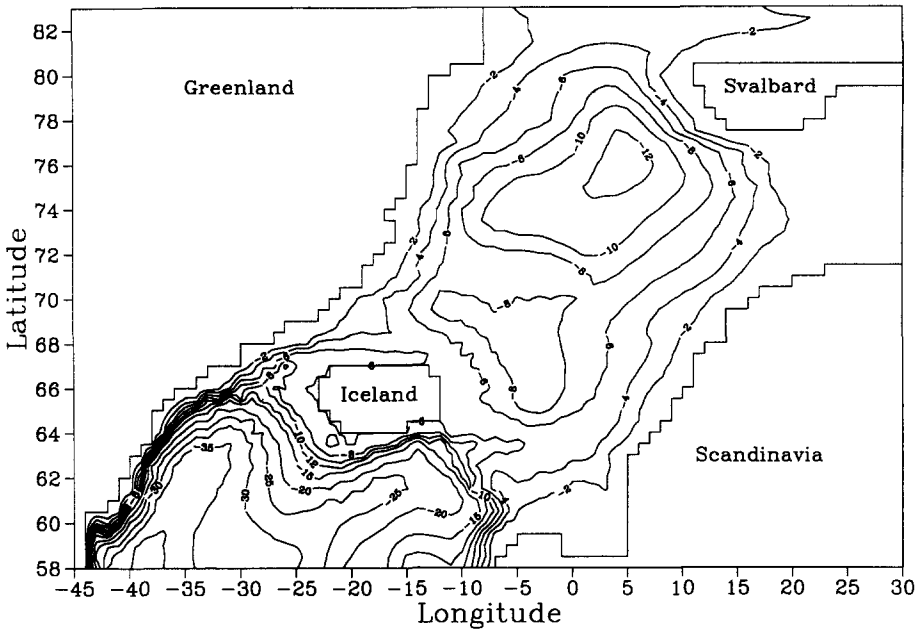


FIG.6. The stream function (in Sverdrups) after 1000 timesteps (31 days) forcing with mean surface data. The contour interval is 2 Sverdrups between -2 and -12 Sverdrups and 5 Sverdrups for values less than -15 Sverdrups.

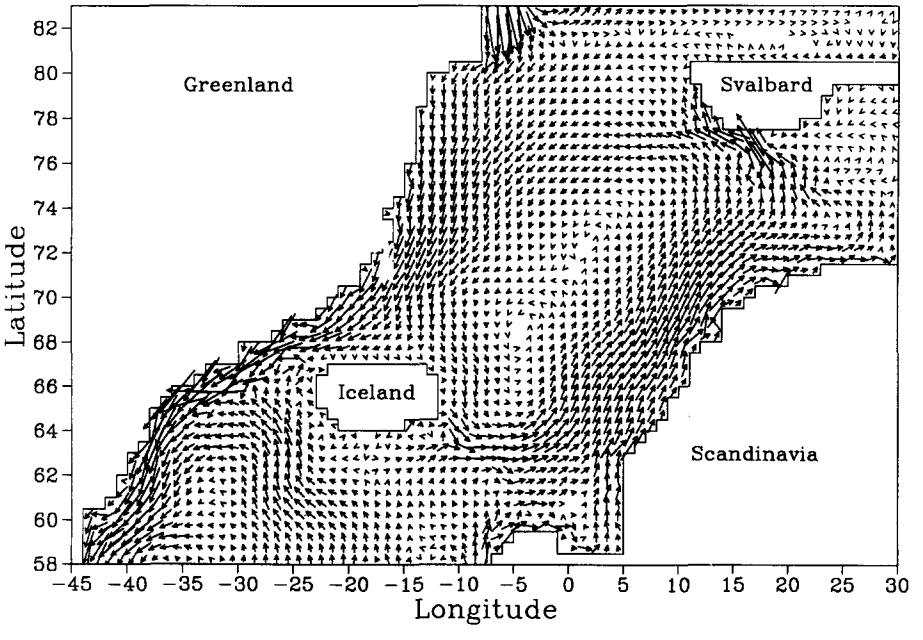


FIG.7. The velocity at level 2 (20m) after five years forcing with mean surface data. The distance between grid points corresponds to a speed of 5cm $s^{-1}$.

caused by the winter cooling which enhances the cyclonic circulation in the Greenland Sea. However, in this case the northward advection of North Atlantic water flattens the isopycnals leading to a less strong Greenland Sea gyre.

The lack of vertical motion in the Norwegian and Greenland Seas is clearly illustrated by the zonally averaged meridional circulation (Fig.9). North Atlantic water can be seen moving northwards at the surface. It passes through the Norwegian and Greenland Seas with very little sinking before moving into the Arctic Ocean. There is a corresponding southward return flow at intermediate depth. No discernible motion occurs deep within the Norwegian and Greenland Seas.

Thus it can be concluded that the use of mean thermohaline forcing is of limited value for studies in the Norwegian and Greenland Seas. The possible exception is for short term studies of wind forcing, where variability occurs on a time scale shorter than it takes the temperature and salinity fields to change significantly. Therefore the response to seasonal forcing is considered next.

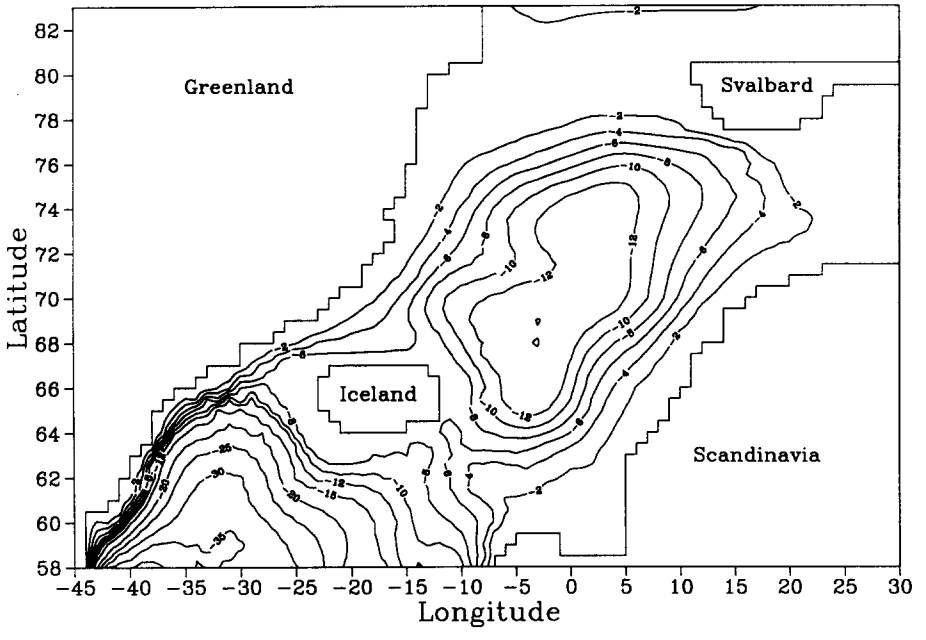


**FIG.8. The stream function (in Sverdrups) after five years forcing with mean surface data. The contour interval is 2 Sverdrups between -2 and -12 Sverdrups and 5 Sverdrups for values less than -15 Sverdrups.**

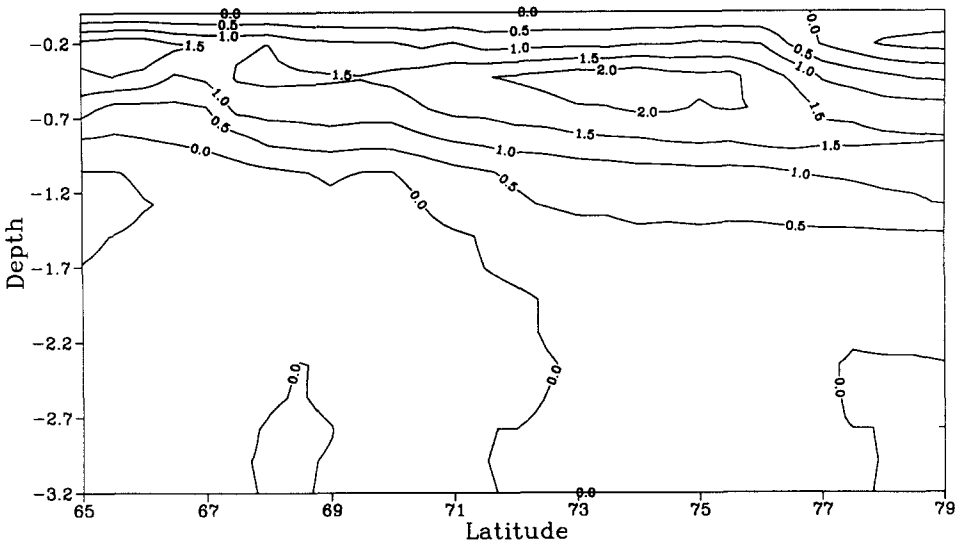


FIG.9. The zonally averaged meridional circulation (in Sverdrups) after five years forcing with mean surface data. The depth is in kilometres.

## 5. A SEASONAL STUDY

### *5.1 Initial and boundary data*

The model described in the previous section has been employed to study the effect of seasonal forcing. The wind stresses used are monthly means derived (as described in section 4) from 12 hourly NMC winds for 1982 and 1983. Linear interpolation is used between each month to capture the seasonal variations while eliminating the high frequency variability that the use of 12 hourly winds produce. A further advantage is that it avoids the excessive computations involved in interpolating each 12 hourly wind onto the model grid. Most of the monthly mean winds are of a similar structure to the annual mean wind (see Fig.4). However there are a few exceptions such as April 1983 (Fig.10).

The thermohaline forcing is taken from an LEVITUS and OORT (1977). This was used because when the work was undertaken it was the only seasonal dataset easily available. Once more the temperature and salinity (and thus density) are prescribed at the sea surface. The surface density for the summer and winter seasons are shown in Fig.11. Comparing these figures with Fig.3 it can be seen that the basic structure of the fields is quantitatively similar to that of the mean data. As would be expected the water is warmer in summer, especially the North Atlantic inflow water that is advected northwards along the Norwegian coast. Also the summer surface water is fresher, presumably as a result of melting sea ice and increased runoff of melt water from land. The winter water is more saline, as a lot of fresh water is locked up in snow and ice and thus is unavailable to freshen the Atlantic inflow to the same extent as in the summer. In the winter the water can be

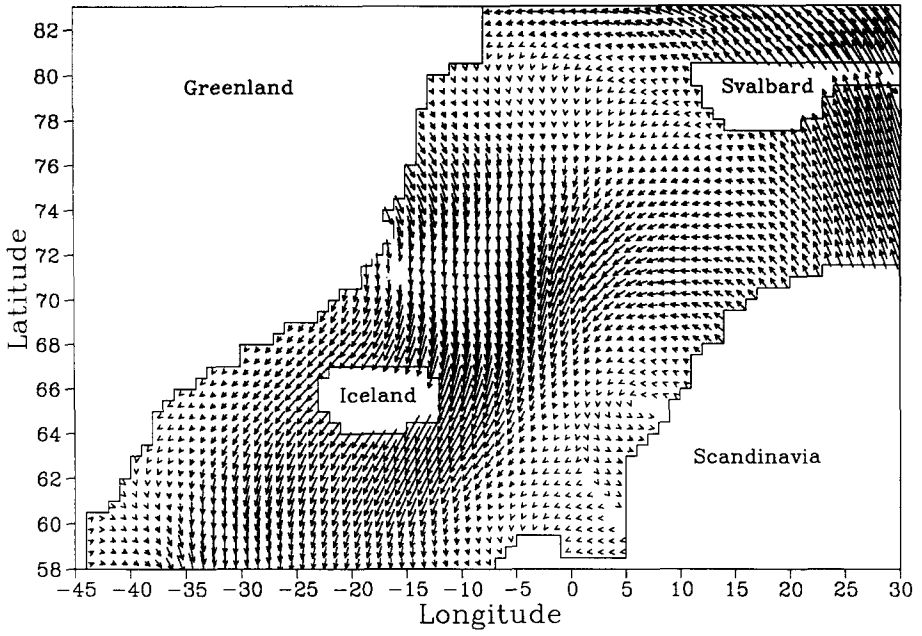


FIG.10. The April 1983 monthly mean wind stress. The distance between grid points corresponds to a stress of $0.1 Nm^{-2}$.

seen to be at its most dense, through the combined effect of lower temperature and higher salinity. Finally it must be pointed out that unlike the mean data used in the previous section these data have not been extensively smoothed. Furthermore they consist of far fewer data points and are rather inaccurate above 75°N. Linear interpolation is used between each season to obtain smooth fields in time. Annual mean values of temperature and salinity are again used in the open boundary condition. In the winter the surface North Atlantic inflow water is dense enough to penetrate at least 100m downwards. In the summer the water restratifies. Thus with the seasonal surface temperature and salinities specified, the variations in these inflows are well represented.

The steady data of the previous section are used to specify the stream function at the open boundaries with the following justification. At the northern boundary the magnitude of the stream function is small. No information is available to accurately specify a seasonal variation. Thus the argument used in section 4, that the budget data of WORTHINGTON (1970) provides a good approximation, is still valid. At the southern boundary density driving, through the bottom pressure torque, is responsible for a large part of the barotropic flow. There should be no large changes in the density field in the region of the boundary. Thus the mean data should provide a good approximation. The forcing at this boundary should at least be consistent with the local topography and density, which appears to be very important in this region. With this approach any distortion to the solution is almost certainly confined to a narrow region close to the boundary.

Once more the model is initialised with the LEVITUS (1982) mean data as it is much smoother and contains more observations than the seasonal data. The model is started from rest and run for fifteen years using the seasonal forcing. For the first fourteen years, 1982 monthly mean winds are used while the last year used 1983 monthly mean winds. This allows the surface and intermediate waters of the ocean to settle into a seasonal cycle. The final year allows the study

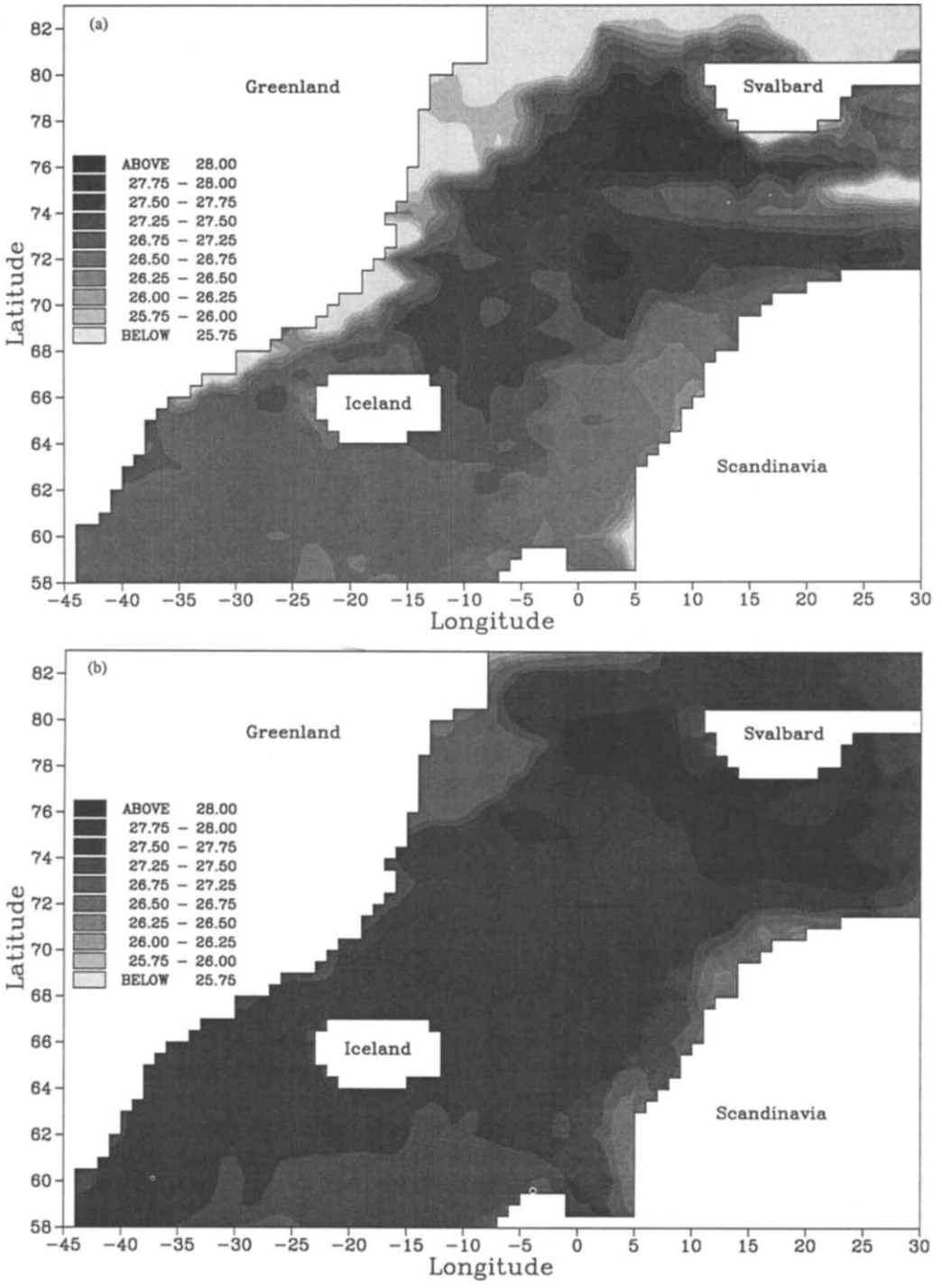


FIG.11. The prescribed surface density for (a) August, September, October and (b) February, March, April. The units are kg $m^{-3}$-1000.

of inter-annual variability caused by the wind forcing. The length of the run makes the results far more prognostic in nature. Results obtained near the initial instant are very much constrained by the initial density field, which stores much of the information about the long term wind driving (HOLLAND and HIRSCHMAN, 1972) and can thus be thought of as semi-diagnostic. All the results described below come from the last two years of the integration which will be referred to as 1982 and 1983.

*5.2 Integrated quantities*

Firstly we consider the barotropic component of the flow which caused the most problems with open boundaries in the previous section. The stream function for November 1982 and May 1983 is illustrated in Fig.12. It can be readily seen that the use of steady barotropic boundary data has caused no real problems. The flow even quite close to the boundary seems to adjust to the varying forcing without any of the unrealistic behaviour that was encountered in Fig.5. Thus the arguments in subsection 5.1 for the use of mean boundary data for the stream function seem justified. The cyclonic circulation associated with the Norwegian and Greenland Seas is always present. A strong gyre exists over the Greenland Sea, whilst weaker circulation extends southward into the Norwegian Sea. This is in contrast to the situation in section 4 where the Norwegian Sea gyre became stronger after five years. Thus it seems that the surface thermohaline forcing has a large part to play in maintaining the barotropic flow over long time scales. The strength of the gyre in the Greenland Sea varies between 13 and 31 Sverdrups with an average of 19 Sverdrups. The cyclonic circulation is even present in May 1983 in spite of the wind producing an anticyclonic Sverdrup flow over the Greenland Sea basin. The mean wind driving produces or enhances a density field consistent with cyclonic circulation. When the wind field is periodically weakened or reverses the density field continues to force the cyclonic circulation, although it may be reduced. Once more it can be seen that topography is important in controlling the circulation. One feature of both figures (and in fact a persistent one) is the very strong West Spitsbergen Current. This is present throughout the run and appears to be produced largely by the seasonal thermohaline forcing. This has been verified by a number of short runs using various combinations of mean and seasonal surface data to drive the model. Figure 13 shows the seasonal cycle of the transport in the Greenland Sea gyre. The largest circulation occurs in the winter months. The figure is comparable to Fig.11 in SEMTNER (1987). The seasonal response is the same, however, the transports are larger here. The size of the gyre in winter is also comparable to the measurements of AAGAARD and COACHMAN (1968).

The model appears to have captured the variability of the exchange of water between the Norwegian and Greenland Seas and the outlying oceans. These exchanges are important quantities from which estimates of both heat and salt transport, which in turn have important consequences for the climate, can be deduced. Many authors have tried to infer values of these transports from observations, for example WORTHINGTON (1970), AAGAARD, DARNALL and GREISMAN (1973), and AAGARD and GREISMAN (1975). For instance it is the inflow of warm saline North Atlantic water into the Norwegian Sea that stops the spread of ice southward on the eastern side of the basin. The northward mass transport (a) across the Scotland-Iceland ridge system and (b) through the Fram Strait, is illustrated in Fig.14. The transport between Scotland and Iceland varies between 3.5 and 13 Sverdrups, with an average of 6.4 Sverdrups. WORTHINGTON (1970) infers that the net northward transport is 6 Sverdrups. WORTHINGTON (1970) infers that the net northward transport is 6 Sverdrups. GOULD (personal communication) suggests the transport to the west of Shetland (the largest component) varies between 4 and 12 Sverdrups, with

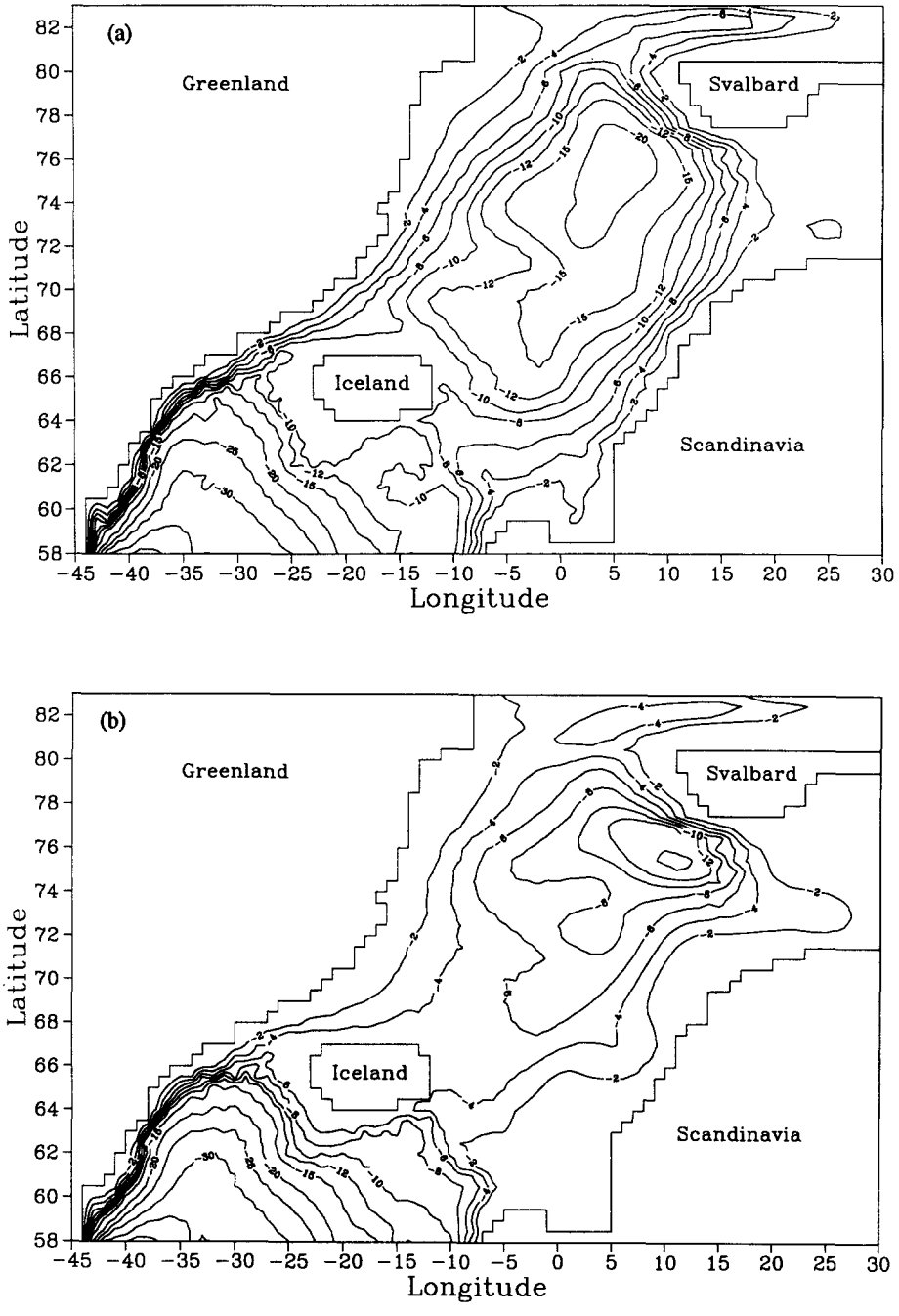


FIG.12. The stream function (in Sverdrups) for (a) November 1982 and (b) May 1983. The contour interval is 2 Sverdrups between -2 and -12 Sverdrups and 5 Sverdrups for values less than -15 Sverdrups.

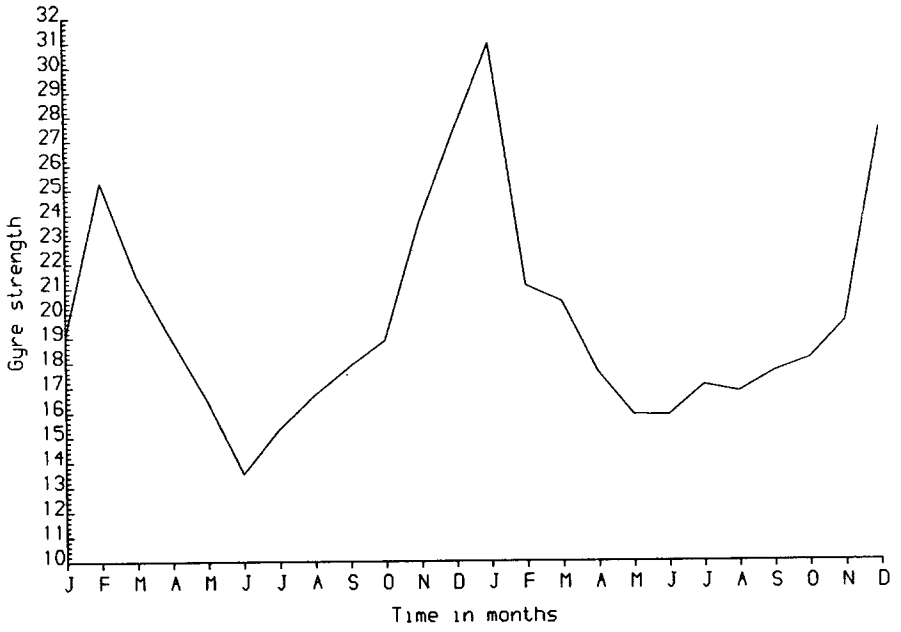


FIG.13. The mass transport (in Sverdrups) of the Greenland Sea gyre from January 1982 to December 1983.

the strongest transports in the winter. In the model the largest northward transport occurs between October and March, while the transport in the summer months is generally weaker. There is considerable inter-annual variability (of which February is a good example) suggesting that the wind is an important factor here. The importance of wind forcing is verified by a homogeneous, non-topographic wind driven calculation in which the variations in transports follow a similar pattern. The transport through the Fram Strait varies between 3.3 and 9.4 Sverdrups with an average of 5.7 Sverdrups. AAGAARD *et al* (1973) estimate an annual mean value of 7.1 Sverdrups based on four long term current meter observations. AAGAARD and GREISMAN (1975) state that a number of investigators have produced estimates from 2 to 8 Sverdrups.

The inter-annual variability of northward heat transport into the Norwegian and Greenland Seas that can be brought about by the wind forcing is illustrated in Fig.15. The figure shows the northward heat transport for February 1982 and 1983. There is a larger northward transport of heat across almost every line of latitude up to 75°N in 1982. This corresponds to a much larger inflow (10.3 Sverdrups compared with 4.7 Sverdrups) from the North Atlantic in 1982. The heat transport in February 1982 is close to the winter value quoted by SEMTNER (1987).

Continuing this theme of northward transports, Fig.16 shows the zonally averaged meridional circulation for February 1982 and September 1983. Unlike the mean circulation (Fig.9) there is now a significant amount of vertical motion in the Norwegian and Greenland Seas. In February North Atlantic water can be seen flowing northwards at the surface before sinking in the Greenland Sea area. This water then returns southwards at depth, flowing over the various ridges and out into the deep North Atlantic. The volume transport of this deep water overflow is approximately 3 Sverdrups, which is in agreement with SWIFT, AAGAARD and MALMBERG

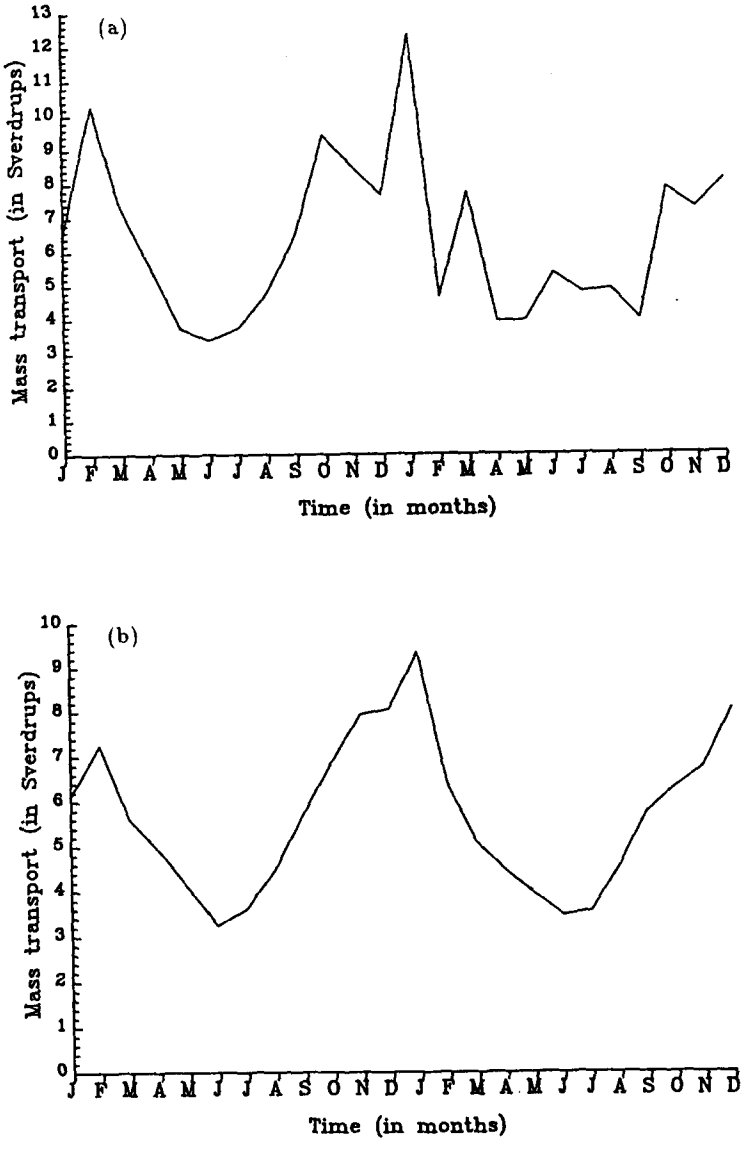


FIG.14. The northward mass transport (in Sverdrups) (a) between Scotland and Iceland and (b) through the Fram Strait, from January 1982 to December 1983.

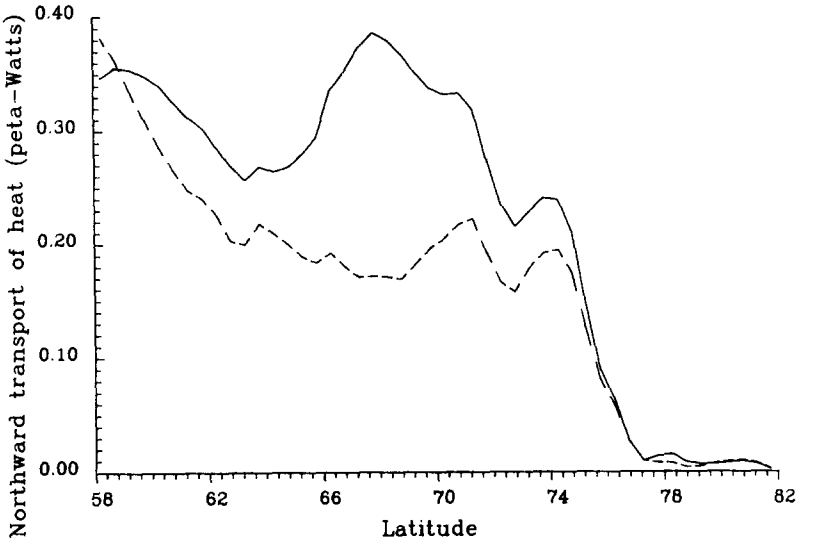


FIG.15. The northward transport of heat (in peta watts) for February 1982 (solid line) and 1983 (dashed line).

(1980). In September there is virtually no northward transport (in this zonally averaged sense) of surface water into the Norwegian Sea. Also the circulation in the vertical is greatly reduced, a feature which is apparent throughout the summer and early autumn. There is variability of the meridional circulation on both seasonal and inter-annual time scales, which suggests the importance of wind driving. For instance in February 1983 (not shown) there is no transport of deep water (in this averaged sense) over the Greenland Scotland ridge; whereas in February 1982 there is the previously noted transport of about 3 Sverdrups.

### *5.3 Horizontal sections*

We now consider horizontal sections of the model results rather than the integrated quantities discussed above. Figure 17 shows the horizontal velocity vectors at level 2 (20m) for February 1982 and 1983. Again these two months are illustrated because of the variability between the two years. Both pictures show that the model has adequately reproduced the known surface currents. A favourable comparison can be made with Fig.1 taken from METCALF (1960). Features present in both years include the strong East Greenland Current which originates in the Arctic Ocean and runs southwards along the Greenland shelf. In February 1982 this current gets particularly strong from the Denmark Strait southward, enhanced by wind driving (this view is supported by a simple barotropic model). On the eastern side of the domain there is a broad northward drift of North Atlantic water most of which follows the shelf north of Norway and flows past Spitsbergen in the West Spitsbergen Current. The remainder of this water flows on to the Barents Sea shelf before rejoining the West Spirsbergen Current. Decomposition of the currents into barotropic and baroclinic components show that the broad northward drift is mainly baroclinic while the West Spitsbergen Current and the flow on the Barents Sea shelf are almost entirely barotropic. Although the West Spitsbergen Current is largely barotropic it appears to be driven by the surface thermohaline forcing. This is easily verified by a few short runs using different combinations of

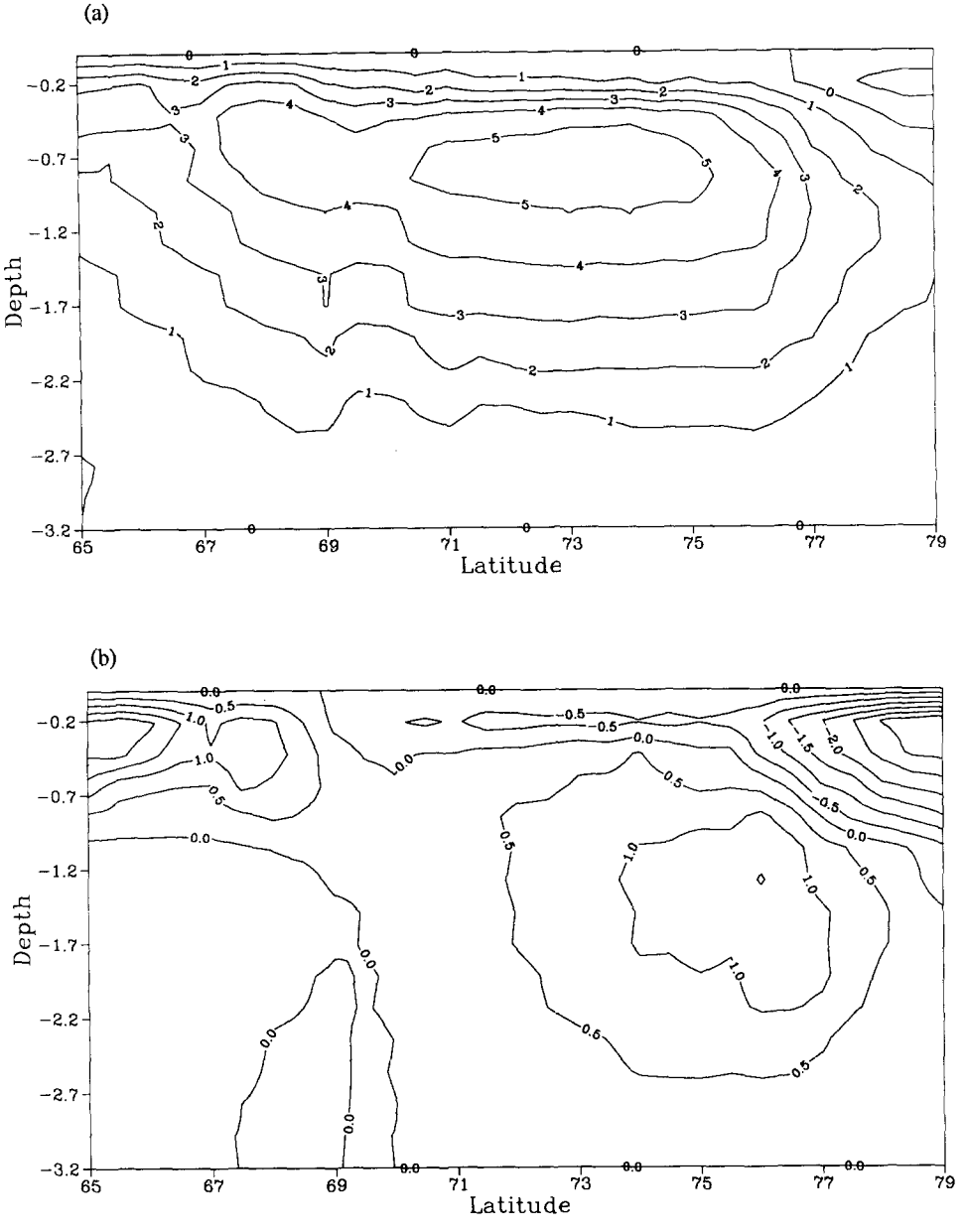


FIG.16. The zonally averaged meridional circulation (in Sverdrups) for (a) February 1982 and (b) September 1983. The depth is in kilometres.

mean and seasonal forcing. The Norwegian Coastal Current is strongly enhanced (by wind driving) in February 1982, when there is a large inflow of North Atlantic water into the Norwegian Sea between Scotland and Iceland. January 1983, another month with a large inflow, had an equally strong coastal current. The observed small inflow of North Atlantic water through the Denmark Strait west of Iceland is modelled. The East Icelandic Current appears in February 1983 but is absent in the previous year. The East Icelandic Current is extremely variable throughout the two years which again suggests it is a wind driven current. Decomposition of the velocity field inciates the East Icelandic Current is a barotropic current.

The surface circulation in one of the summer months, August 1983, is shown in Fig.18. Many of the main features described above are again present. However there are detail differences between all three sets of surface currents. For instance, in August 1983 the inflowing North Atlantic water meanders toward and away from the Norwegian coast at approximately 67°N. This is caused by the density field, which has a corresponding kink toward the coast in the isopycnals. This feature also occurs in the August 1982 current. Other months have their own distinctive current patterns caused by the density field as well as inter-annual features caused by the varying wind stress. Such patterns in the currents re-occur year after year. Herein lies one of the disadvantages of rigorously imposing the surface tracer field. The imposed density gradients can drive currents through the pressure term in the momentum equations that are as large or larger than all other effects. Cyclonic circulation persists in the surface flow throughout the region and in smaller cells over each basin for the full length of the integration. With reference to Fig.2 the controlling effect that topography has on the surface currents can always be seen in the circulation patterns.

Attention is now turned to deeper currents. Figure 19 shows the horizontal velocity field at level 8 (520m) for January 1983. This is just above the level of the sills between the Norwegian Sea and the North Atlantic. There is always outflow from the Norwegian Sea at the deepest level of the Denmark Strait. This is not unexpected as the mass transport here is always southward. However this is not necessarily always dense overflow water. What is surprising is that there is always a strong outflow between the Faroes and Iceland even though the mass transport here is always northward. This is even true in January 1983 when the northward transport is exceptionally large, although it must be stated that the strength of the outflow is reduced. This outflow water which is more dense than the surrounding water, sinks as it passes over the ridge and can be traced travelling westward to the South of Iceland before flowing into the North Atlantic. There is also a deep outflow between the Faroes and Scotland in some months although this is weaker and far more intermittent. This flow, when it exists, turns in a clockwise direction around the Faroes and moves toward the Iceland-Faroes outflow. In reality it is thought (SWIFT *et al*, 1980) that the main and persistent outflow of Norwegian Sea deep water between Scotland and Iceland is through the Scotland-Faroes Channel. This is the deepest connection between the Norwegian and Greenland Seas and the North Atlantic. However in the smoothed Levitus topography of the model it is no deeper than the Iceland-Faroes ridge, which is somewhat wider at depth. This helps to explain the persistent deep outflow in the Iceland-Faroes Channel. This hypothesis has since been confirmed by the initial results from a higher resolution model which is under development. The currents induced in the central regions of the domain vary on a seasonal basis as a result of the changes in wind forcing. The circulation is strongest in the winter months and generally at its weakest in the spring and summer. The cyclonic features of the circulation at this level are always maintained. A southward flowing undercurrent is noticeable along the edge of the Norwegian shelf in some months. The West Spitsbergen Current is still quite intense at this depth, displaying its barotropic nature. In Fig.19 it can be clearly seen that the East Greenland Current splits into

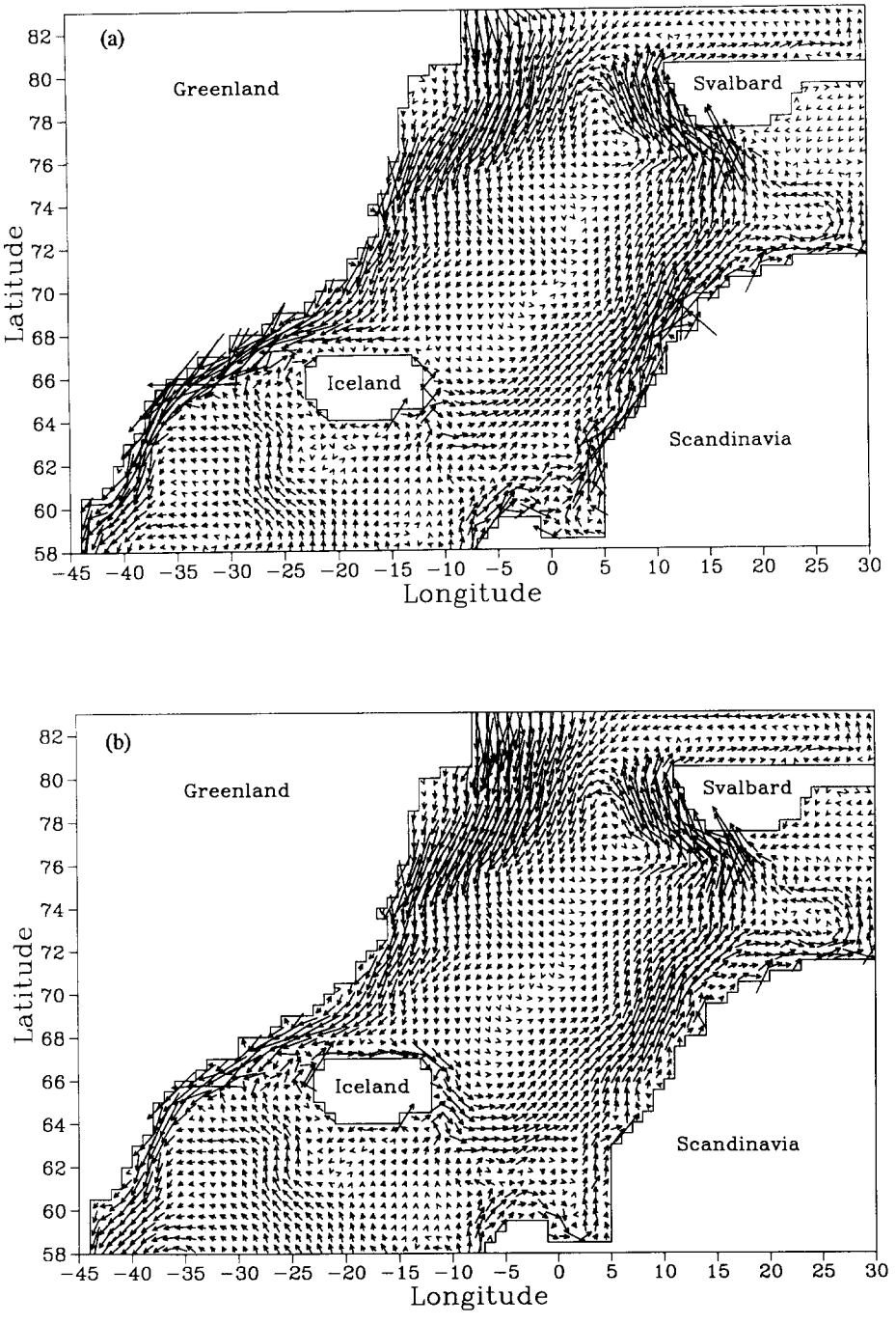


FIG.17. The horizontal velocity at 20m for (a) February 1982 and (b) February 1983. The distance between grid points corresponds to a speed of 5cm $s^{-1}$.

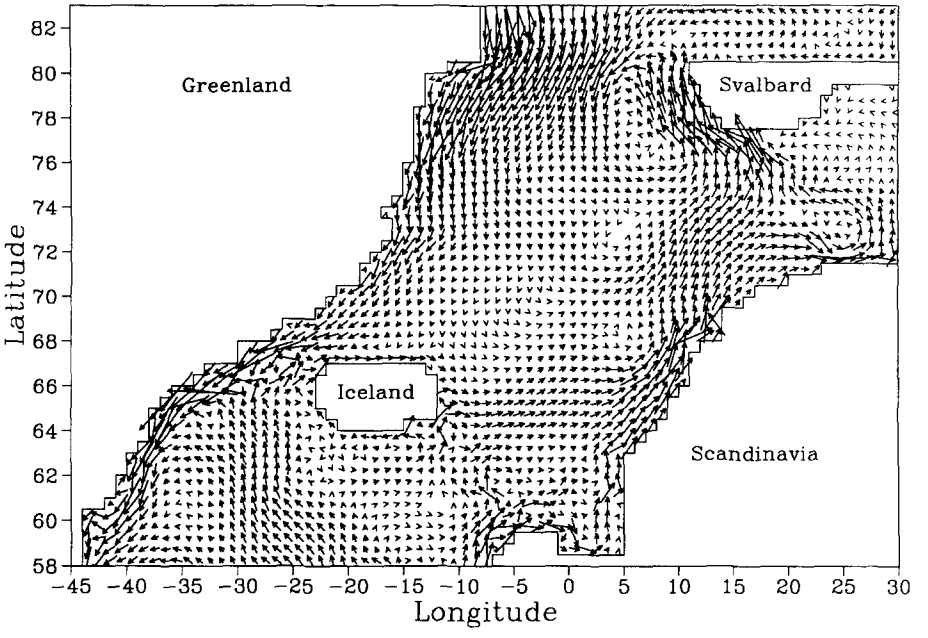


FIG.18. The horizontal velocity at 20m for August 1983. The distance between grid points corresponds to a speed of 5cm $s^{-1}$ velocities.

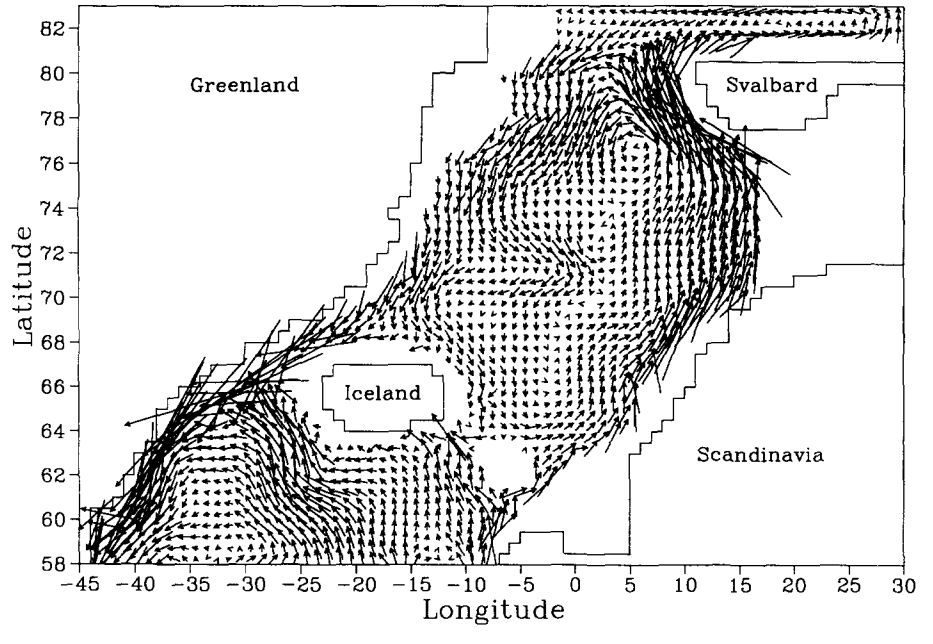


FIG.19. The horizontal velocity at 520m for January 1983. The distance between grid points corresponds to a speed of 2cm $s^{-1}$.

two branches as it flows southwards from the Arctic Ocean. One branch continues southward along the Greenland shelf while the other follows the Jan-Mayen Ridge. Further south there is another split with the two branches passing either side of Iceland.

We now continue deeper by considering the currents at level 11 (1400m). Figure 20 shows the currents at this level for November 1982 and February 1983. There is a considerable amount of seasonal (and in fact inter-annual) variation at this level, which indicates the important effect of wind forcing. Persistent features include the northward moving deep West Spitsbergen Current and the southward flow on the western side of the Greenland Sea. The southward current in the more central portion of the Greenland Sea is smaller in February 1983 than November 1982 and all but vanishes by May of that year. This is almost certainly a consequence of the wind forcing. As mentioned above, it is trying to induce anticyclonic circulation over the Greenland Sea. This explains why the southward flow has moved toward the eastern side of the Greenland Sea basin. In February 1983 there is a southwards moving undercurrent along the southern edge of the Barents Sea shelf. Further south in the Norwegian Sea the situation is even more variable, southward flow sometimes occurring on the western side of the basin and sometimes on the eastern side. The flow tends to be on the western side from October to April (for the two years modelled) but this is not always the case. Again southward flow dominates.

Turning now to level 14 (2600m) the currents are still variable on both seasonal and inter-annual time scales. Thus it seems that the wind forcing can have an effect on the deepest waters. Figure 21 shows the currents for November 1983. The circulation in the Greenland Sea can only be described as southward. However, at other times the circulation is cyclonic. Currents in the Norwegian Sea tend to be cyclonic in the winter months and southward in the summer months.

An illustration of the surface or near surface temperature, salinity or density fields would be of little value as they are strongly constrained by the surface boundary condition. In fact the basic structure is very much as one would expect given the imposed boundary conditions. It is of greater interest to look at vertical sections of the tracer fields. However for completeness two horizontal sections at deeper levels will be shown. Figure 22(a) illustrates the temperature field at level 8 (520m) for November 1982. The structure is very much as expected given the surface forcing, with the warmest water in the south and east and the coldest water in the north and west. Points of note are the inflow of North Atlantic water which is advected northwards along the Norwegian coast, Barents Sea shelf and past Spitsbergen before entering the Arctic Ocean. This water forms a wedge that is inclined in towards the coast. Warmer water penetrates further north in the summer months. The water over the Greenland Sea basin is always less than 0°C, with the warmer inflow water skirting around the basin. This is in contrast to the run with mean surface forcing where warming occurred, as there was no vertical convection and cooling of the water in this region. Tight fronts exist across the narrow gaps separating the Norwegian Sea from the North Atlantic, the sharpest is at the Iceland-Faroes ridge. Comparing with Fig.3(b) it can be seen that there is no large deviation from the initial temperature field. However the field has become less smooth. Furthermore, the path of the warm North Atlantic water is more consistent with the known currents than the initial field. Figure 22(b) shows the salinity at the same time and depth. The structure of the isohalines are similar to the isothermals in the previous figure. The saline North Atlantic water is advected northwards along the Norwegian coast, while fresher water from the Arctic Ocean is advected southwards along the Greenland side of the sea. Comparing with Fig.3(c) it can be seen that the salinity of the North Atlantic inflow has become more consistent with the current system. Patches of high salinity water are apparent to the West of Spitsbergen. This is caused by the poor quality of the surface boundary data. The surface water in this region is forced cold, saline and thus very dense. This water sinks and spreads out contaminating the deep waters of both the Norwegian and Greenland Seas with water of higher salinity than occurs in reality.

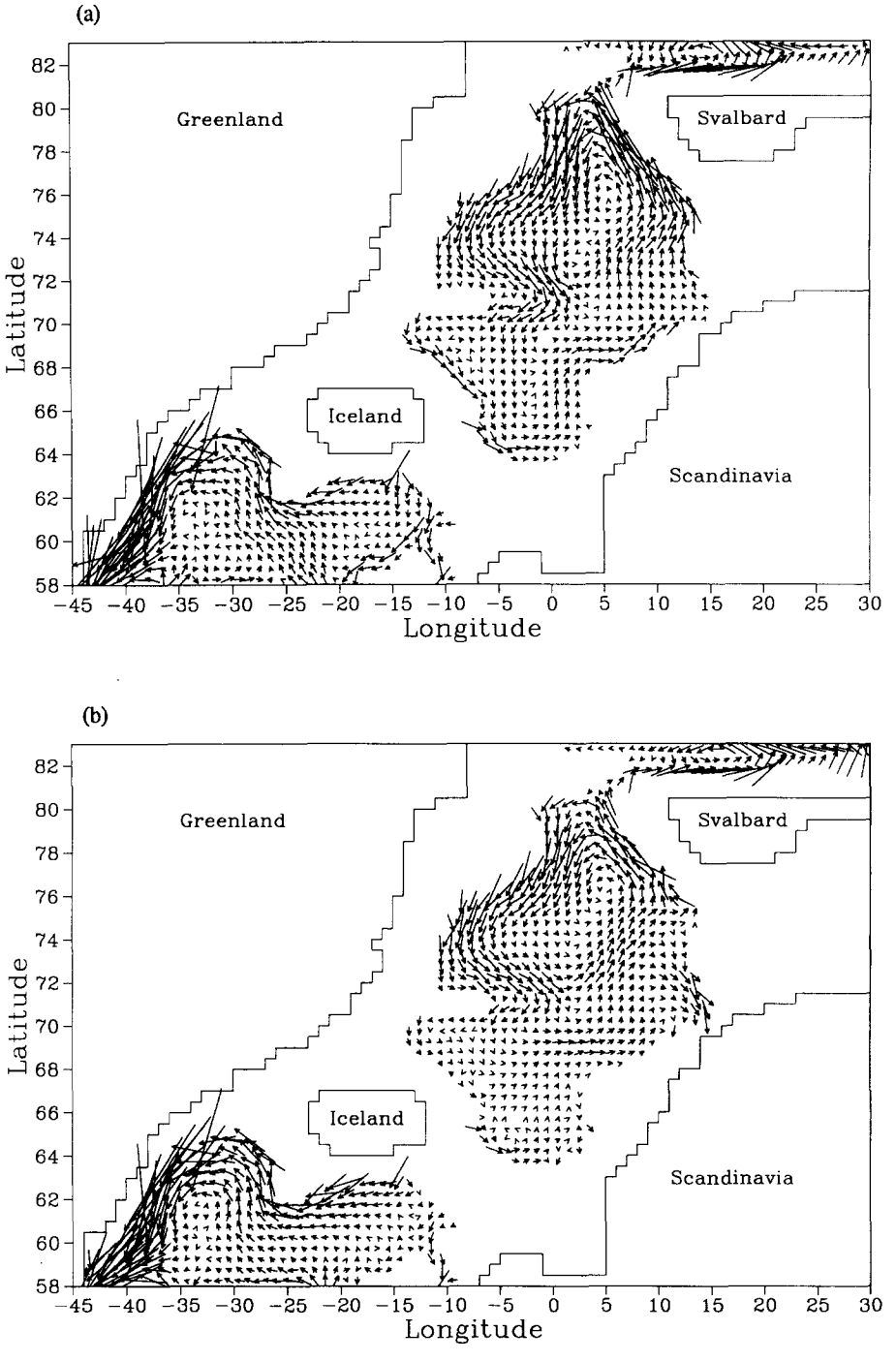


FIG.20. The horizontal velocity at 1400m for (a) November 1982 and (b) February 1983. The distance between grid points corresponds to a speed of 1cm $s^{-1}$.

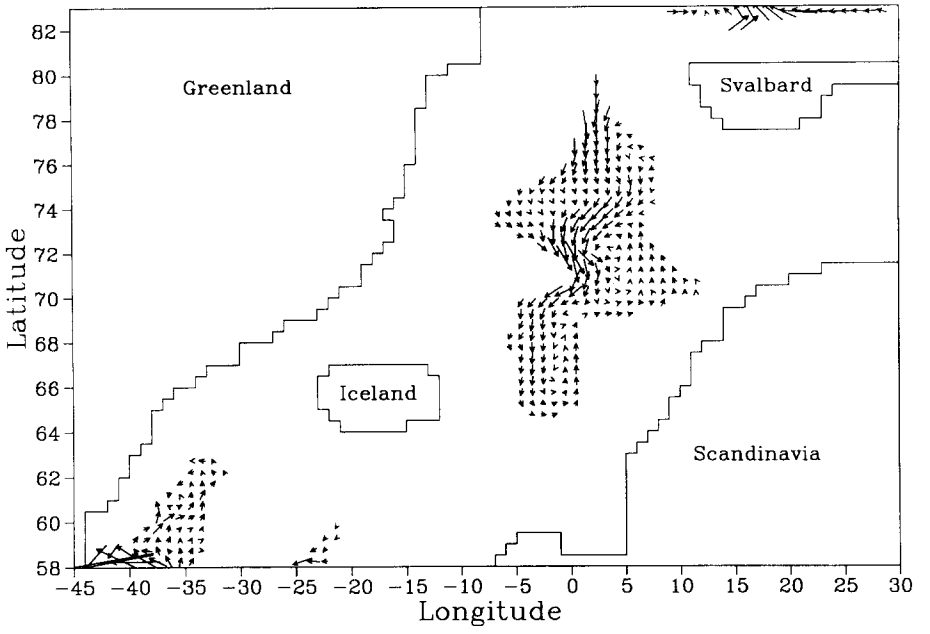


FIG.21. The horizontal velocity at 2600m for November 1983. The distance between grid points corresponds to a speed of 1cm $s^{-1}$.

### *5.4 Vertical sections*

Finally attention is turned to vertical sections. Figure 23 shows a north-south section of temperature at 10°E for March 1983. All the expected features occur, including warm surface water in the south and cooler water to the north. The subsurface core of North Atlantic water moving along the Norwegian coast can be clearly seen (as indicated by the 7°C water). In the north the -1°C water indicates a region of convective mixing. The cold surface water mixes down to about 1200m.

East-west temperature and salinity sections at 66°N for August and February 1983 are illustrated in Fig.24. The two pictures give a good indication of the movement of water masses. The temperature section shows northwards moving Atlantic water (<8°C), leading onto the continental shelf of Norway to a depth of about 400m. The structure of this wedge is very similar to that observed by HORN and SCHOTT (1976). Further west the water is cooler, with only a shallow warmer layer near the surface. Much of the deep water is nearly isothermal, as is observed by LEE (1963). Immediately to the West of Iceland (in the Denmark Strait), North Atlantic water can be seen moving northwards. Further west is the cold East Greenland Current. Deep in the western corner cold (<0°C) water can be seen tilted up against the Greenland coast. This is water of deeper origin that is pushed up over the sill. The tilting up against the coast is caused by the effect of the Earth's rotation (GILL, 1982, p.390). The picture of salinity illustrates several well known features. Moving from west to east, firstly there is the low salinity, East Greenland Current water adjacent to the Greenland coast. To the west of Iceland, northward-moving Atlantic water can be observed, of which the core has sunk beneath lighter fresh water. To the east of Iceland is the relatively fresh, southward-moving East Icelandic Current water. Further east is the main

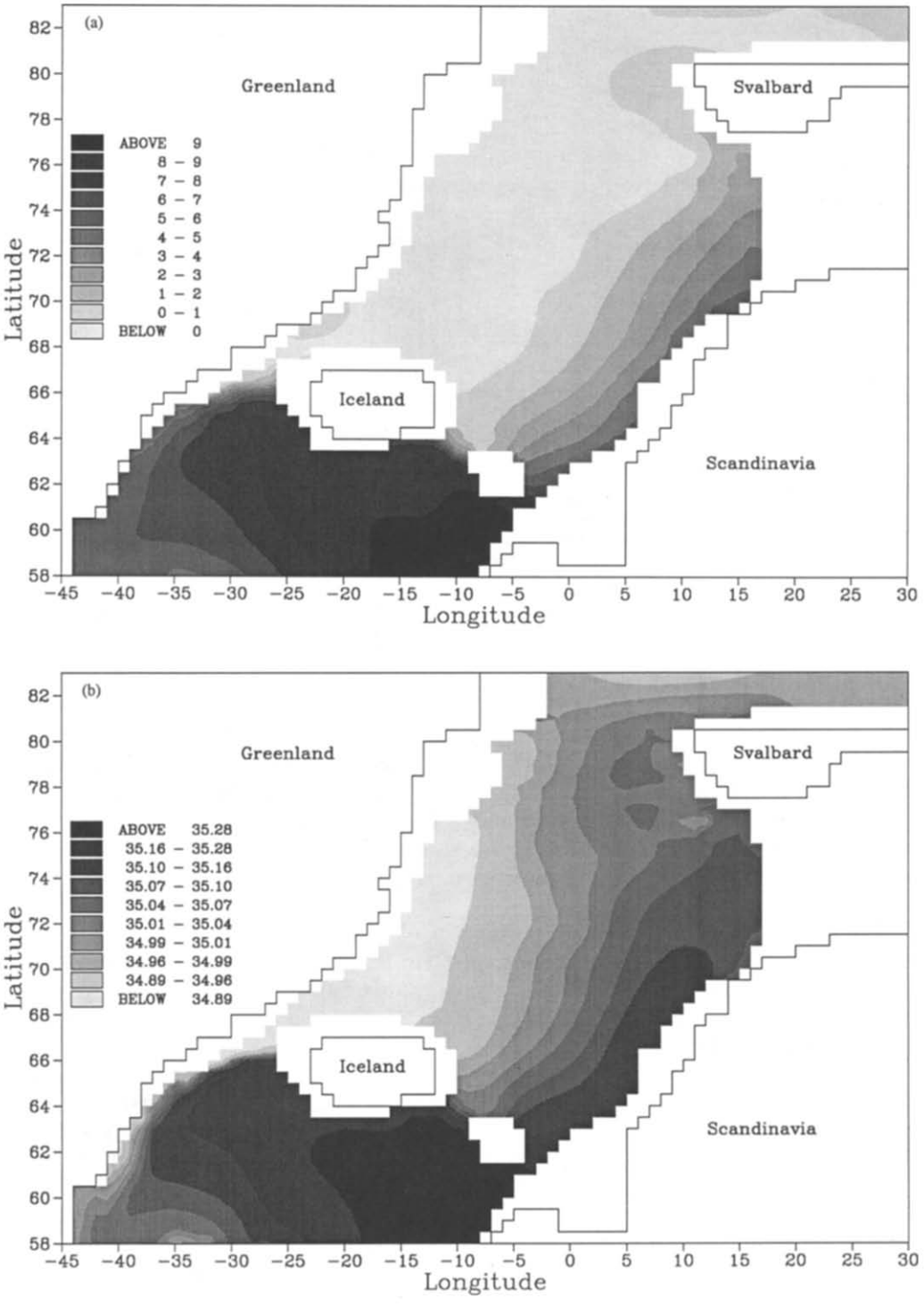


FIG.22. The (a) temperature (°C), and (b) salinity (ppt) at 520m for November 1982.

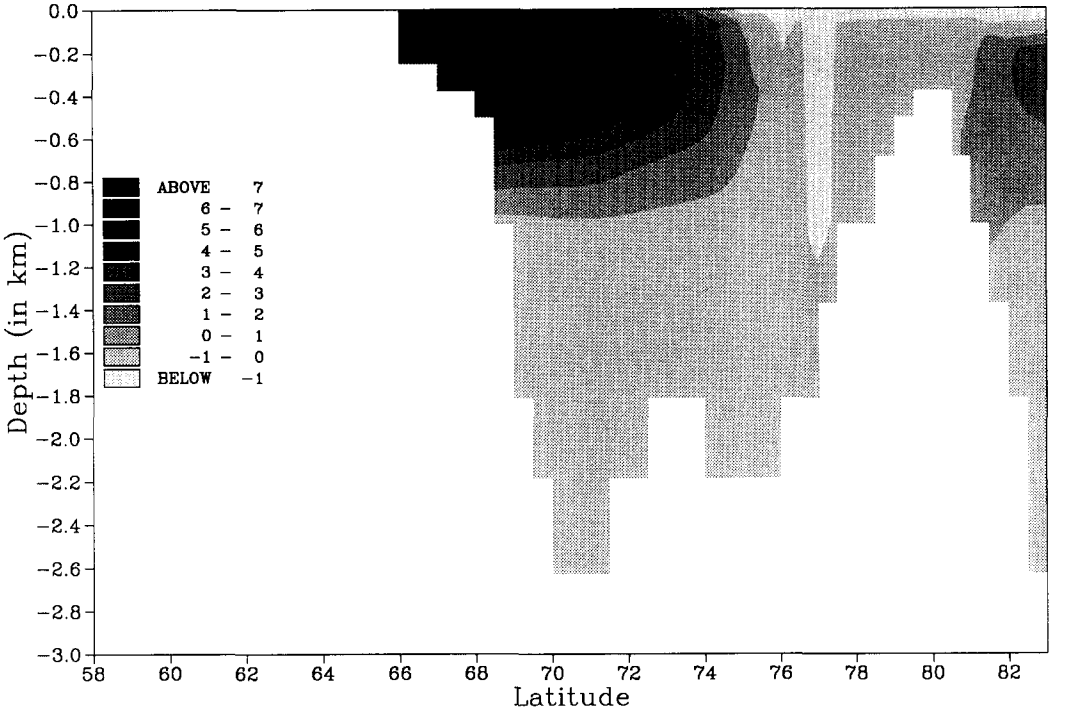


FIG.23. A north-south temperature (°C) section at 10°N for March 1983.

bulk of northward-moving North Atlantic water. Again this water leans onto the Norwegian continental slope, where it is overlain by fresh coastal runoff water. The effect of coastal runoff is well reproduced by specifying salinity at the sea surface. The deepest water is of salinity greater than 35 ppt rather than the observed water of about 34.92 ppt, which is caused by the process mentioned at the end of section 5.3. The behaviour of the water masses is very similar to that suggested by HSIEH and GILL (1984). The Atlantic water moves along the eastern coasts and the Norwegian Sea water moves along western coasts. Each water mass travels with the coastline on its right, controlled by the rotation of the Earth.

We now examine a section at 69.5°N, which cuts across the northern part of the Norwegian basin. Figure 25 shows the density field in November 1982. Lighter (fresher) water is apparent at the coasts. In the interior of the basin, the familiar doming up of isopycnals, which enhances the cyclonic circulation, is evident. The northward velocity at this section is illustrated in Fig.26 for May and November 1982. The basic feature of northward flow in the East and southward flow in the West is present in both pictures. However, there is considerable variability. In May there is a stronger northward flow of Atlantic water and a weaker southward flow of polar water than in November. In May the centre of the Atlantic water is pushed off the coast and a southwards flowing undercurrent hugs the Norwegian continental slope, but in November this undercurrent is absent. However, the undercurrent occurs in other months, for instance May 1983 when the picture is almost identical to that in May 1982. This suggests density effects may be dominant here (or that the mean wind was very similar in both years). However an undercurrent is apparent in February 1983, but not in 1982 when there was a particularly large transport northward into the

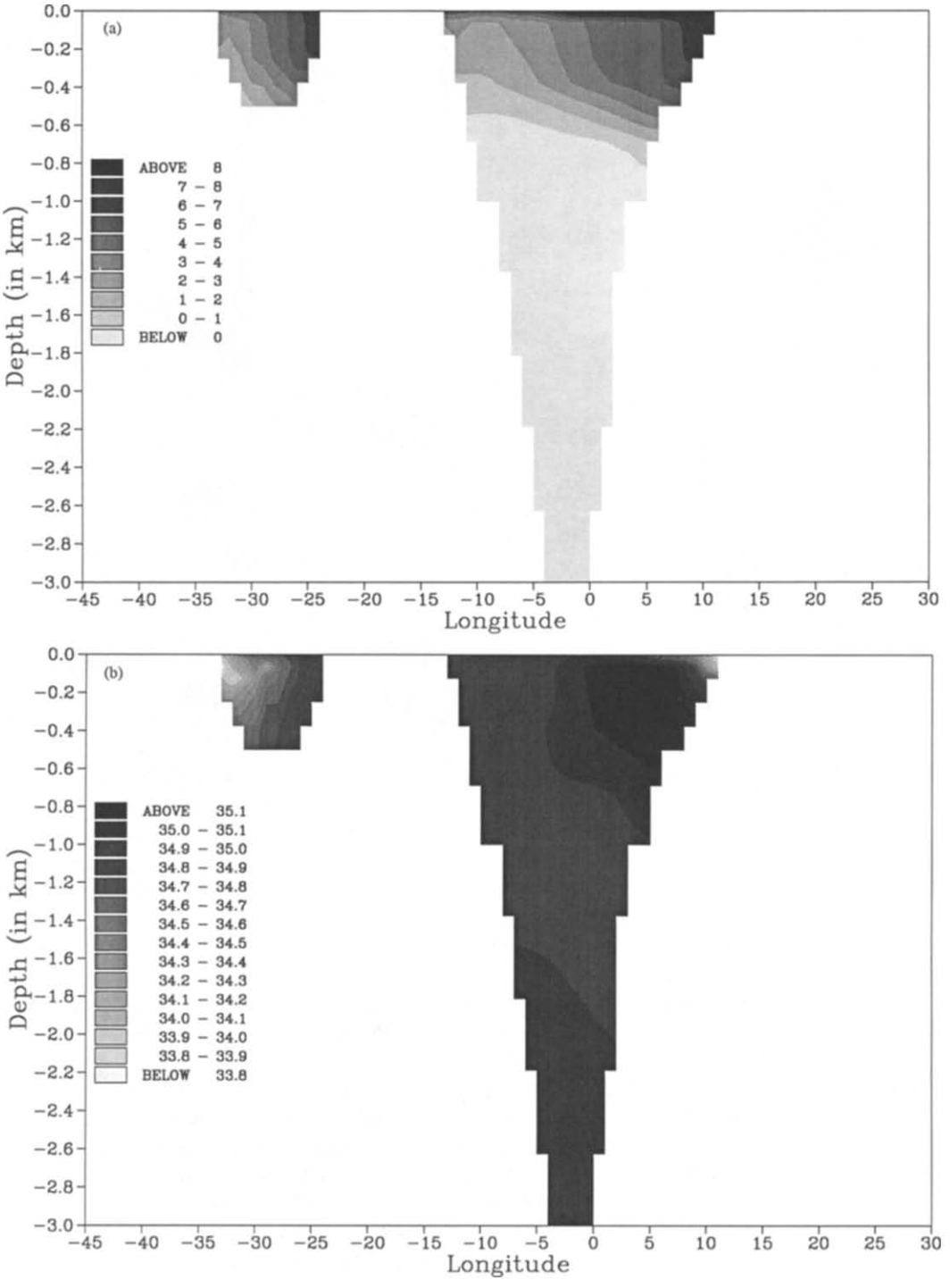


FIG.24. An east-west section at 66°N of (a) temperature (°C) in August 1983 and (b) salinity (ppt) in February 1983.

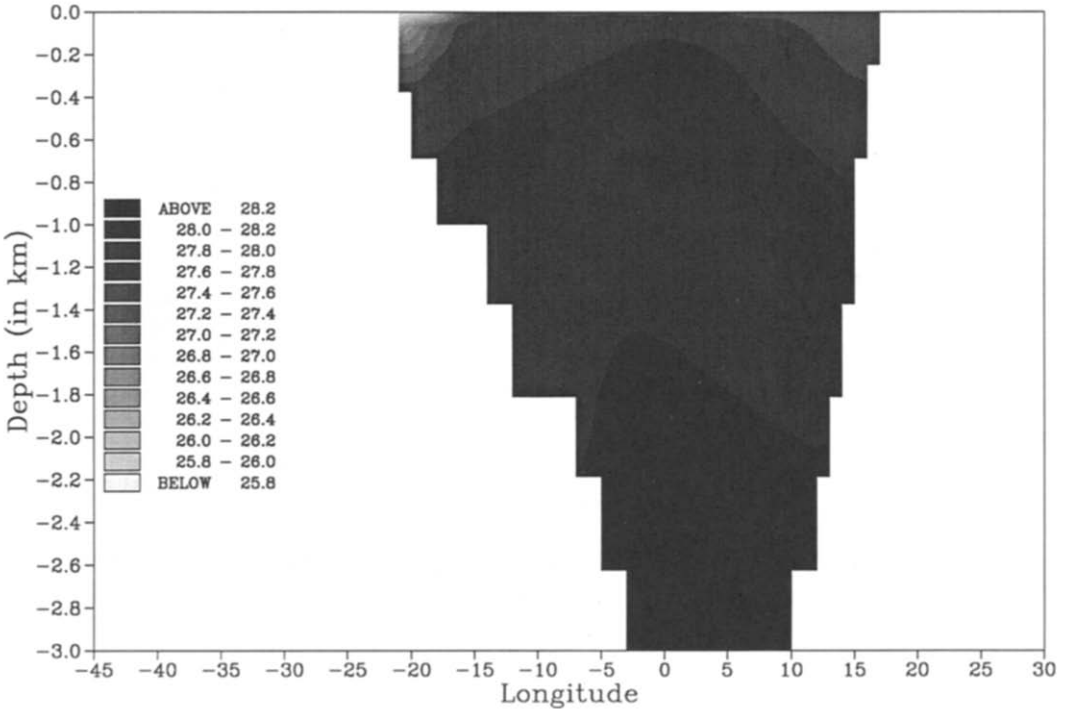


FIG.25. An east-west section at 69.5°N of density $\sigma_\theta$ (kg $m^{-3}$-1000) in November 1982.

Norwegian Sea. Thus the wind driving has an important part to play. In November there is a much smaller northward undercurrent to the East Greenland Current just off the Greenland continental slope. This undercurrent occurs in other months but is always very small.

Finally we look at a section through the Greenland and Barents Seas at 75.5°N. Figure 27 shows the temperature in February 1982. Over the Barents Sea shelf-break the remains of the warm North Atlantic inflow water can be seen as it is advected into the West Spitsbergen Current. In the centre of the basin the isothermals dome upwards, indicating that there is a cyclonic circulation and surface cooling. The cold surface East Greenland Current can be seen adjacent to the Greenland coast, with beneath it a warmer undercurrent which is thought to exist (LEE, 1963). Figure 28 shows the northward velocity at this section for November 1982. The Greenland Sea basin is split into two distinct parts with northwards moving water in the east and southwards moving water in the west. The extremely strong current over the Barents Sea shelf-break is the start of the West Spitsbergen Current. To the west the surface intensified East Greenland Current can be seen against the Greenland coast. The situation here is very similar from month to month, with the main variations being in the strength of the currents.

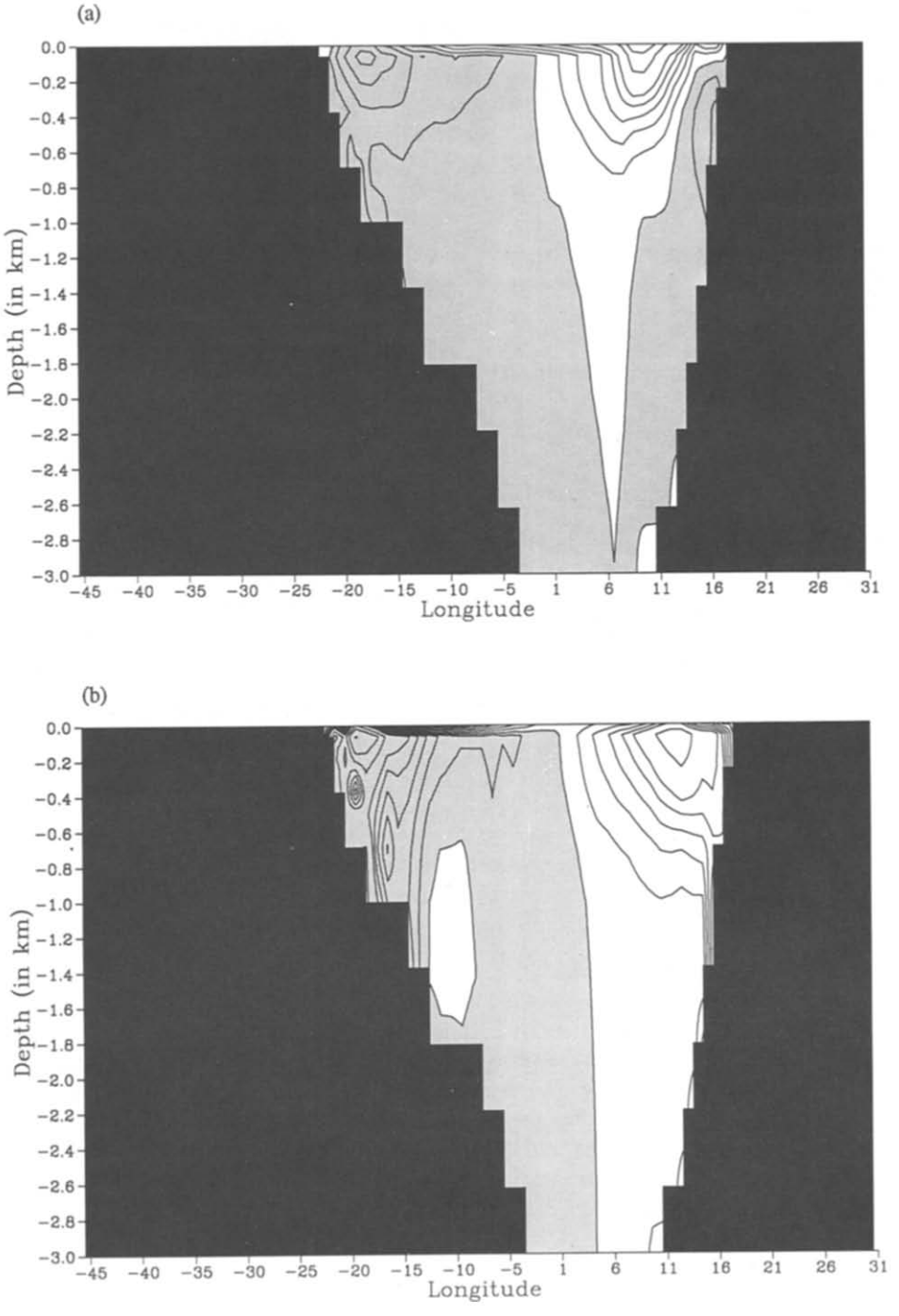


FIG.26. The northward velocity (in cm $s^{-1}$) at 69.5°N for (a) May 1982 and (b) November 1982. Southward flow is shaded. The contour interval is 0, 61, 62, 63, 64, 65, 67.5, 610, 615, 620cm $s^{-1}$.

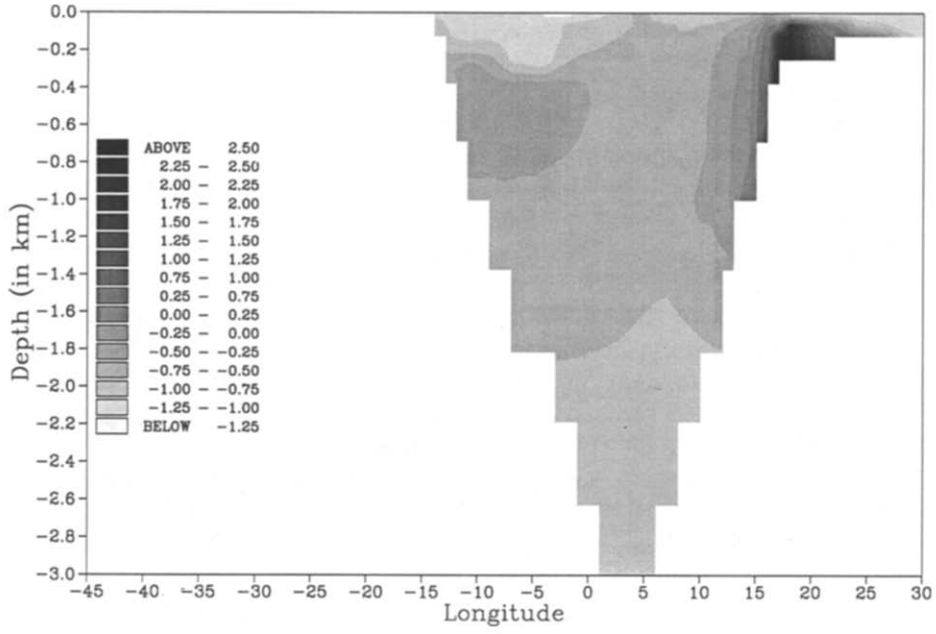


FIG.27. An east-west temperature (°C) section at 75.5°N for February 1982.

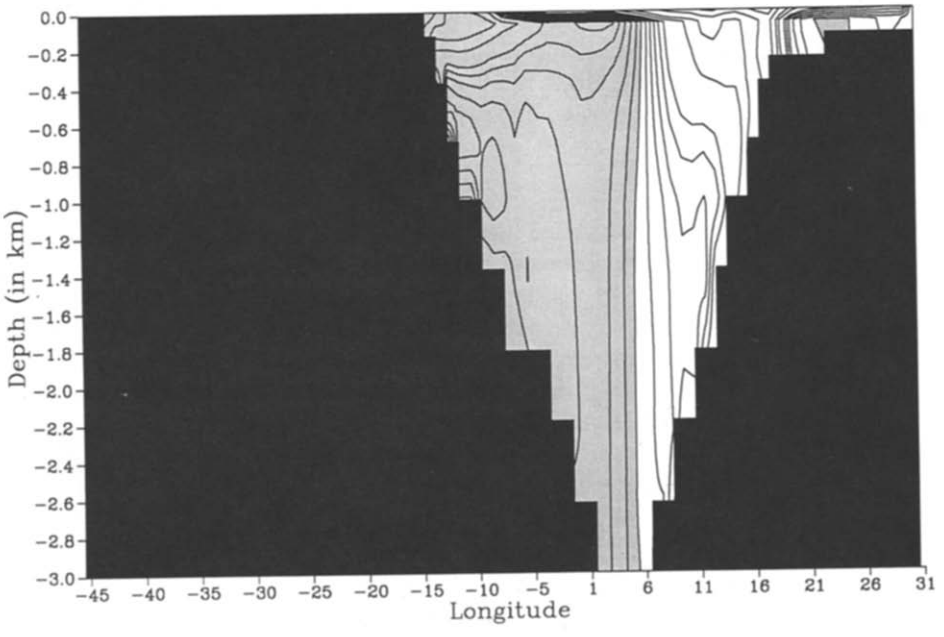


FIG.28. The northward velocity (cm $s^{-1}$) at 75.5°N for November 1982. Southward flow is shaded. The contour interval is 0, 61, 62, 63, 64, 65, 67.5, 610, 615, 620cm $s^{-1}$.

## 6. CONCLUSION AND FUTURE IMPROVEMENTS

The Norwegian and Greenland Seas have been studied using a primitive equation ocean circulation model. In its final form the model is driven by inflows and outflows from the surrounding oceans and seasonally varying wind, temperature and salinity forcing at its surface. Many of the observed features of the temperature and salinity fields and currents have been reproduced. It is clear from the present results that both seasonal buoyancy and wind driving are important if the circulation is to be realistically modelled. Thus the use of such a complex model which retains most of the physics describing ocean circulation is justifiable.

Modellers are always going to be in difficulty when confronted with open boundaries. In general, the values of variables at open boundaries are dependant both on what is happening inside and outside the model domain (which is unknown). Observations need to be blended with information from the interior of the model to provide a best possible picture. Reasonable and consistent arguments can be put forward concerning the treatment of the baroclinic mode and tracers at open boundaries. However the barotropic mode, by the nature of the complex equation describing it, is far more troublesome. No useful, easily obtainable solutions are available except in the simplest of situations. A pragmatic approach has to be taken in using whichever method works best in each given situation.

Better results could be achieved with this model if better forcing data could be used. At present the surface data used gives inaccurate deep water formation, which leads to the deep water becoming anomalously saline. Improved simulation can be expected through using seasonally varying fluxes of heat and salt at the sea surface, as real oceans are driven by fluxes. A flux condition would allow the surface waters far more freedom and would be a much greater test of the model. However, even if heat fluxes are obtained, for instance using air temperatures from meteorological analysis, evaporation minus precipitation data of reasonable accuracy are unlikely to be available for some time. Thus salinity will still have to be designated at the sea surface from oceanographic datasets. However it would probably be better to relax the surface salinity to the data (rather than rigorously imposing it) by adding a term

$$\alpha(S_{ob} - S_1)$$

to the right hand side of the tracer equation (5) describing salinity; where $\alpha$ is the e-folding time for the forcing and $S_{ob}$ and $S_1$ are the observed and model surface salinities.

If flux data are used, an ice model will be required to allow ice formation, for otherwise unrealistically low temperatures may be generated. A simple parameterisation of the type used by SEMTNER (1976b) will reproduce the insulating effect of ice cover and provide a crude prediction of the ice edge. More complex models of the type used by HIBLER (1979) or SEMTNER (1976a) could be used, which will give far more accurate prediction of the ice edge and ice thickness.

The present runs indicate that the effect of topography is very important. However, the topography used was taken from the LEVITUS (1982) dataset, which is highly smoothed and stored in 1° grid boxes. The use of unsmoothed (or partially smoothed) topography from a higher resolution dataset is thus desirable. Greater horizontal resolution would not only enable some of the ridges and other topographic features (at present poorly represented) to be properly resolved, but also resolve oceanographic eddies. Thus if the grid size were to be reduced to a half or even better to a quarter of its present size, then this interesting new physics would be brought within the scope of the model.

Finally the treatment of vertical mixing in the present generation of three dimensional primitive equation models is in need of substantial improvement. Tests by the author involving a number of different parameterisations for vertical mixing show that the resulting horizontal circulation is sensitive to the method used. Tests by KILLWORTH (1990) have shown how poorly the convection process (which is obviously crucial at high latitude) is represented in these models.

## 7. ACKNOWLEDGEMENTS

The author wishes to thank Dr John Johnson for much useful discussion during the course of this work. The work was completed in 1988/89 under NERC grant GR3/6716.

## 8. REFERENCES

AAGAARD, K. (1970) Wind-driven transports in the Greenland and Norwegian seas. *Deep-Sea Research*, **17**, 281-291.

AAGAARD, K. and L.K. COACHMAN (1968) The East Greenland Current north of Denmark Strait, Part I. *Arctic*, **21**, 181-200.

AAGAARD, K. and P. GREISMAN (1975) Toward new mass and heat budgets for the Arctic Ocean. *Journal of Geophysical Research*, **80**, 3821-3827.

AAGAARD, K., C. DARNALL and P. GREISMAN (1973) Year-long current measurements in the Greenland-Spiutsbergen passage. *Deep-Sea Research*, **20**, 743-746.

ANDERSON, D.L.T. and P.D. KILLWORTH (1977) Spin-up of a stratified ocean, with topography. *Deep-Sea Research*, **24**, 709-732.

ASSELIN, R. (1972) Frequency filter for time integrations. *Monthly Weather Review*, **100**, 487-490.

BRYAN, K. (1969) A numerical method for the study of the circulation of the World ocean. *Journal of Computational Physics*, **4**, 347-376.

BRYAN, K. and M.D. COX (1972) An approximate equation of state for numerical models of Ocean circulation. *Journal of Physical Oceanography*, **2**, 510-514.

BRYAN, K., S. MANABE and R.C. PACANOWSKI (1975) A global-atmosphere climate model. Part II. The oceanic circulation. *Journal of Physical Oceanography*, **5**, 30-46.

CARMACK, E. and K. AAGAARD (1973) On the deep water of the Greenland Sea. *Deep-Sea Research*, **20**, 687-715.

COX, M.D. (1984) *A primitive equation, 3-dimensional model of the ocean.* GFDL Ocean Group Technical Report No.1.

CREEGAN, A. (1976) A numerical investigation of the circulation in the Norwegian Sea. *Tellus*, **28**, 451-459.

GILL, A.E. (1982) *Atmosphere-Ocean Dynamics*. Academic Press, London, 662pp.

HIBLER, W.D. (1979) A dynamic thermodynamic sea ice model. *Journal of Physical Oceanography*, **9**, 815-846.

HIBLER, W.D. and K. BRYAN (1987) A diagnostic ice-ocean model. *Journal of Physical Oceanography*, **17**, 987-1015.

HOLLAND, W.R. and A.D. HIRSCHMAN (1972) A numerical calculation of the circulation in the North Atlantic Ocean. *Journal of Physical Oceanography*, **2**, 336-354.

HOPKINS, T.S. (1988) The Gin Sea, Review of the physical oceanography and literature from 1972. *Saclantcen SR-124*, La Spezia, SACLANT ASW Research Centre.

HORN, W. and F. SCHOTT (1976) Measurements of stratification and currents at the Norwegian continental slope. *Meteor Forschungsergebnisse*, Reihe A, **18**, 23-63.

HSIEH, W.W. and A.E. GILL (1984) The Rossby adjustment problem in a rotating, stratified channel, with and without topography. *Journal of Physical Oceanography*, **14**, 424-437.

KILLWORTH, P.D. (1979) On "chimney" formations in the ocean. *Journal of Physical Oceanography*, **9**, 531-554.

KILLWORTH, P.D. (1989) On the parameterisation of deep convection in ocean models. In: *'Aha Huliko'a Winter workshop on parameterisation of small-scale processes*, P. MULLER, editor, University of Hawaii, 59-74.

KILLWORTH, P.D., J.M. SMITH and A.E. GILL (1984) Speeding up ocean circulation models. *Ocean Modelling*, **56**, 1,4.

LEE, A. (1963) The hydrography of the European Arctic and Subarctic Seas. *Oceanography and Marine Biology Annual Review*, **1**, 47-76.

LEGUTKE, S. (1987) The influence of boundary conditions on the circulation in the Greenland-Norwegian Sea. A numerical investigation. In: *Three-dimensional models of marine and estuarine dynamics*, J.C.J. NIHOUL and B.M. JAMART, editors, Elsevier, Amsterdam, 269-283.

LEVITUS, S. (1982) *Climatological atlas of the world ocean*. NOAA Publ.13, US Department of Commerce, Washington, DC, 173pp.

LEVITUS, S. and A. OORT (1977) Global analysis of oceanographic data. *Bulletin of the American Meteorological Society*, **58**, 1270-1284.

METCALF, W.G. (1960) A note on water movement in the Greenland-Norwegian Sea, *Deep-Sea Research*, **7**, 190-200.

O'BRIEN, J.J. (1986) The diffusive problem. In: *Proceedings of the NATO Advanced Study Institute on Advanced Physical Oceanographic Numerical Modelling*, J.J. O'BRIEN, editor, D. Reidel Publishing Co., Dordrecht, 127-144.

PETERSON, W.H. and C.G.H. ROOTH (1976) Formation and exchange of deep water in the Greenland and Norwegian Seas. *Deep-Sea Research*, **23**, 273-283.

SEMTNER, A.J. (1974) *An oceanic general circulation model with bottom topography*. UCLA Department of Meteorology Technical Report No.9,. 99pp.

SEMTNER, A.J. (1976a) A model for the thermodynamnic growth of sea ice in numerical investigations of climate. *Journal of Physical Oceanography*, **6**, 379-389.

SEMTNER, A.J. (1976b) Numerical simulation of the Arctic Ocean circulation. *Journal of Physical Oceanography*, **6**, 409-425.

SEMTNER, A.J. (1986) Finite-difference formulation of a world ocean model. In: *Proceedings of the NATO Advanced Study Institute on Advanced Physical Oceanographic Numerical Modelling*, J.J. O'BRIEN, editor, D. Reidel Publishing Co., Dordrecht, 187-202.

SEMTNER, A.J. (1987) A numerical study sea ice and ocean circulation in the Arctic. *Journal of Physical Oceanography*, **17**, 1077-1099.

STEVENS, D.P. (1990) On open boundary conditions for three dimensional primitive equation ocean circulation models. *Geophysical and Astrophysical Fluid Dynamics*, **51**, 103-133.

SWIFT, J.H., K. AAGAARD and S. MALMBERG (1980) The contribution of the Denmark Strait overflow to the deep North Atlantic. *Deep-Sea Research*, 27, 29-42.

WORTHINGTON, L.V. (1970) The Norwegian Sea as a Mediterranean basin. *Deep-Sea Research*, **17**, 77-84.